2008-01-25

Sedimentological and Biological Analyses on Hobble Creek Prior to Restoration

Jaron Michael Brown
Brigham Young University - Provo

SEDIMENTOLOGICAL AND BIOLOGICAL ANALYSES ON HOBBLE CREEK PRIOR TO RESTORATION

by

Jaron M. Brown

A thesis submitted to the faculty of

Brigham Young University

in partial fulfillment of the requirements for the degree of

Master of Science

Department of Civil and Environmental Engineering

Brigham Young University

April 2008

BRIGHAM YOUNG UNIVERSITY

GRADUATE COMMITTEE APPROVAL

of a thesis submitted by

Jaron M. Brown

This thesis has been read by each member of the following graduate committee and by majority vote has been found to be satisfactory.

Date	Rollin H. Hotchkiss, Chair
Date	Russell B. Rader, Member
Date	Alan K. Zundel, Member
Date	Mark C. Belk, Member

BRIGHAM YOUNG UNIVERSITY

As chair of the candidate's graduate committee, I have read the thesis of Jaron M. Brown in its final form and have found that (1) its format, citations, and bibliographical style are consistent and acceptable and fulfill university and department style requirements; (2) its illustrative materials including figures, tables, and charts are in place; and (3) the final manuscript is satisfactory to the graduate committee and is ready for submission to the university library.

Date

Rollin H. Hotchkiss
Chair, Graduate Committee

Accepted for the Department

E. James Nelson
Graduate Coordinator

Accepted for the College

Alan R. Parkinson
Dean, Ira A. Fulton College of Engineering and Technology

ABSTRACT

SEDIMENTALOGICAL AND BIOLOGICAL ANALYSES

ON HOBBLE CREEK PRIOR

TO RESTORATION

Jaron M. Brown

Department of Civil and Environmental Engineering

Master of Science

Hobble Creek is one of several inflowing streams and rivers into Utah Lake, Utah, USA. Historically, June sucker (*Chasmistes liorus*), a federally listed endemic fish, spawned up all the major inflowing streams and rivers but is now limited to just the Provo River. The State of Utah has recently proposed restoring the lower reaches of Hobble Creek for additional spawning and rearing needs. This restoration effort will likely involve removal of migration barriers, re-aligning the stream, and removing existing levees that prevent floodplain access. These changes have raised several questions that this study aims to answer. First, what are the sediment transport rates under current flow conditions in Hobble Creek, and how well do various predictive

models match the actual rates? Secondly, assuming a successful introduction of adult June sucker into the Hobble Creek system, will the existing flow regime be capable of transporting the fry to an area adequate for successful population growth?

Four bedload predictive models were used to create sediment rating curves for flows typically found in Hobble Creek: the Meyer-Peter, Muller equation (MPM), Wilcock's two parameter model, Rosgen's Pagosa reference curve, and Bathurst's Phase 2 equation. Each were used and compared to data obtained on Hobble Creek during the spring 2006 snowmelt runoff season. Results show that the uncalibrated MPM formula over predicted bedload rates by several orders of magnitude, while the Wilcock model sometimes performed more accurately, but was also prone to inaccuracies greater than an order of magnitude. The Rosgen and Bathurst predicted rates were consistently within an order of magnitude of observed rates.

Areas of optimal rearing potential were determined by separating the stream-lake interface into four zones: dense vegetation, sparse vegetation, open lake, and within the creek. These four zones were analyzed for rearing potential based on food resources, temperature patterns and existing small fish densities. Larval drift modeling was performed to characterize the ability of the stream to transport larvae to the zones studied. We found that highest food density occurs in the open lake; small fish were most abundant in the open lake as well. The open lake is also better for rearing habitat in terms of temperatures between zones. Furthermore, larval drift studies show that the current geometry and flow regime is incapable of transporting larvae to zones in the lake where food and warm water are both available, and that larvae are likely to die before reaching those areas.

ACKNOWLEDGMENTS

I wish to thank Dr. Rollin Hotchkiss for his frequent advice and for his example- both professionally and personally. I am also very grateful to the members of my graduate committee: Alan Zundel, Mark Belk, and Russ Rader for their helpful guidance and suggestions along the way. Huge thanks to our team of undergrad students: Aaron Beavers, John Aedo, Mark Morris, Shawn Stanley, Tammy Thompson, and Joe Webb for their terrific job getting the field work done, counting what, at the time, seemed to be endless amounts of zooplankton, and tremendous help in data reduction and presentation preparation. This research work has been a great experience in teamwork and cooperation, thanks to them. And to Jess, my wife, who kept me well fed and well slept while this research was underway: there is no way I could have done this project without her support.

TABLE OF CONTENTS

LIST OF TABLES

LIST OF FIGURES

1 On The Importance of Field Data in Determining Sediment Transport Rates in Hobble Creek

Chapter Abstract

Bedload transport data are both time consuming and costly to collect. Many predictive models are used to forgo the costs that physically measuring bedload rates can add to a restoration project. The objective of this study is to show that not only are predictive equations prone to differ from actual transport rates, but that those differences can result in vastly different channel design dimensions. Bedload data were obtained on Hobble Creek, Utah in the spring of 2006. Four predictive models were used to predict bedload rates: the Meyer-Peter, Müller (MPM) formula, Wilcock's two parameter model, Rosgen's Pagosa reference curve, and Bathurst's Phase 2 bedload transport equation. Observed rates were compared to predicted rates, and sediment transport at bankfull conditions was used to find stream design geometries (width, depth, and slope). The MPM formula consistently over predicted the transport rates by several orders of magnitude; this resulted in narrow, deep stream designs. The Wilcock, Rosgen, and Bathurst models generally performed better, although bedload rates up to two orders of magnitude larger than observed rates were predicted at some sites. Design geometries based on the Wilcock, Rosgen, and Bathurst bedload rates were similar to those geometries designed to carry observed transport rates. This indicates that simply choosing a sediment transport model in hopes of reducing costs and designing restored

channels for predicted rates will not work. Predictive equations may be less expensive than collecting bedload data, but the increased risk of incorrect channel dimensions and a resulting channel failure should create a sufficient incentive for restoration engineers to seriously consider collecting bedload data in the field.

1.1 Introduction

The practice of obtaining bedload data in the field for stream restoration projects is not always used in consulting engineering firms; in fact, current literature (Doyle et al 2007) on the subject has hinted that using predictive equations rather than field data is the norm amongst restoration firms due to economic and time constraints. The objective of this paper is to show the relevance of obtaining field data and the vast differences between final channel design dimensions based on predictive models and channel dimensions based on field data.

1.2 Bedload Measurements

Bedload transport data were collected at several locations on Hobble Creek during the spring 2006 snowmelt runoff season (see Figure 1-1). The flowrate peaked at 13.3 m^3/s (representing approximately a 5 year flood) and decreased daily down to 2.1 m^3/s, at which point bedload movement ceased. Bedload traps designed by Bunte and Abt (Bunte et al 2007) of the United States Forest Service were used to obtain bedload samples, and the total transport rate of the stream was found and correlated with the measured flow rate that occurred on each sampling day.

1.2.1 Measurement Sites

Measurement sites were selected based on two criteria. The highest priority was given to sites where uniform flow conditions existed. Hobble Creek is an ungaged stream; consequently, discharge measurements were needed with every bedload measurement, so the hydraulic characteristics at each site needed to be such that an accurate discharge measurement could be taken. The second criterion in selecting sites was proximity to roads and/or bridges; these being necessary for bedload sampling during unwadeable conditions. Roads facilitated the delivery of several portable bridges designed and constructed to span the stream only a few feet above the water surface (see appendix for bridge details). Data from three sites were used in this study; Figure 1-1 depicts Hobble Creek and the relative locations of these sample sites.

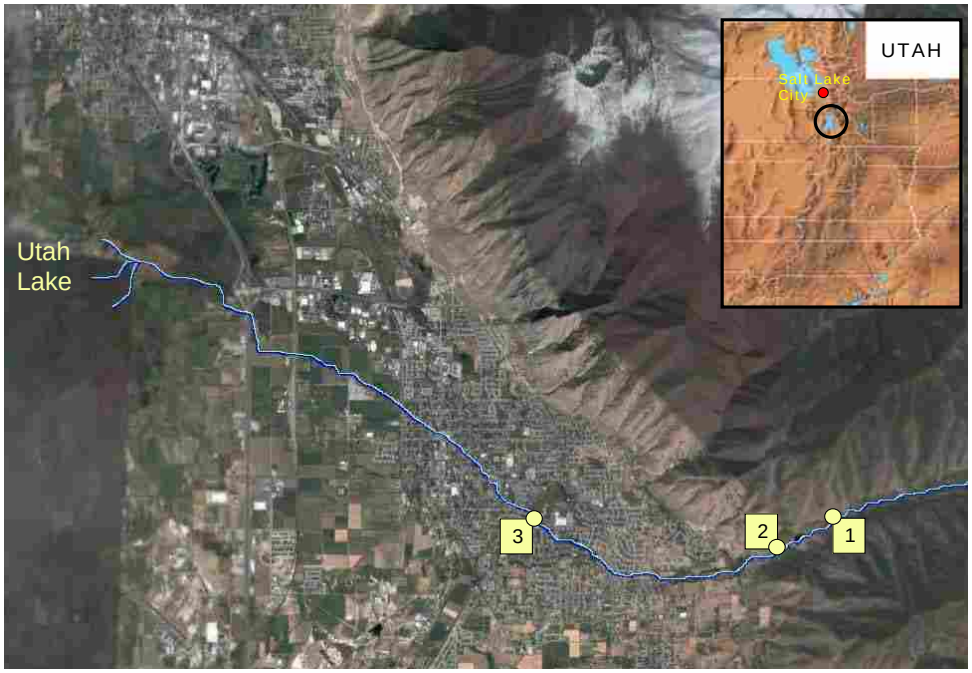

Figure 1-1. Hobble Creek flows through Springville Utah into Utah Lake. Sample Sites are labeled according to their relative location on Hobble Creek.

1.2.2 Sampling Methods

Bunte/Abt traps were used to collect bedload data. These traps have an opening of 0.30 m, and a 4.5 mm mesh net. A ground plate, designed to improve sampling efficiency, was staked to the streambed below each trap. Wadeable conditions are required before bedload measurements begin in order to set up ground plates and the stakes to which the traps are attached. In Figure 1-2 one of the Bunte-Abt traps is shown as it would have appeared on the streambed.

Figure 1-2. One of 12 Bunte-Abt traps built and deployed at sample Sites 1-4.

When conditions were such that wading in the stream to set up the Bunte/Abt traps was unsafe or impossible, a hand-held variation of the Bunte/Abt traps was used. This variation, known as the "Stanley Sampler" incorporated several sections of steel pipe that, when coupled together, form a forked pole up to 12' long; this was attached to the Bunte/Abt traps using the straps normally used to fasten the trap to the ground stakes

(see Figure 1-3). All sampling devices were used in a similar fashion, by measuring the width of the stream and taking samples at evenly spaced intervals across the stream. Thus, only a percentage of the streambed width was sampled. Sample times ranged from 5 minutes to 1 hour, depending on the stream flow rate and rate at which the sampler nets would fill up. When flows and bedload were high, sample times longer than 5 minutes resulted in nets too heavy to pull out easily, but once the flow subsided sample times up to an hour long were required to collect bedload. Data from bedload sampling is summarized below in Table 1-1.

Figure 1-3. This hand-held variation of the Bunte-Abt trap requires no wading.

Table 1-1. Summary of bedload transport, hydraulic, surface and subsurface data used in this study.

Location	date	discharge (cfs)	sample weight (g)	sample time (min)	bed width (ft)	Sampling Device	Sampler Width (ft)	# of samples	slope (ft/ft)	D_{65} surface (mm)	D_{50} surface (mm)	D_{50} subsurface (mm)	Ave. Depth (ft)
Site 1	11-May	266.1	29.2	5	19	Stanley	1	7	0.007	80	61	16	2.38
Site 1	18-May	248.4	1724.7	5	18	Stanley	1	11	0.007	80	61	16	2.20
Site 1	27-May	160.9	0.5	10	16	Stanley	1	10	0.007	80	61	16	1.82
Site 1	31-May	98.7	0.01	60	18	B/A	1	5	0.007	80	61	16	1.61
Site 2	23-May	196.7	4	5	23	Stanley	1	15	0.015	98	69	27	1.55
Site 2	25-May	140.9	1795.7	5	23	B/A	1	7	0.015	98	69	27	1.34
Site 2	31-May	89.5	73.94	60	23	B/A	1	7	0.015	98	69	27	1.01
Site 3	17-May	304.5	1726.4	5	22	Stanley	1	14	0.028	90	75	1.5	2.06
Site 3	19-May	240.7	366	5	22	Stanley	1	14	0.028	90	75	1.5	1.85
Site 3	24-May	155.2	12.55	5	22	Stanley	1	13	0.028	90	75	1.5	1.53
Site 3	30-May	103.2	626.76	60	22	B/A	1	8	0.028	90	75	1.5	0.75
Site 3	1-Jun	80.6	1.3	60	16	B/A	1	4	0.028	90	75	1.5	0.58

1.2.3 Transport Rate Calculation

Equation [1-1] was used to find the calculated bedload transport rate in L^3T^{-1}:

$$Q_s = \frac{MB}{twn\rho s} \quad \textbf{[1-1]}$$

where:

Qs = Bedload Transport Rate (L^3T^{-1})

M = Total mass caught in traps (M)

B = Streambed Width (L)

t = sample time (T)

w = sampler width (L)

n = number of traps

ρ = density of water (ML^{-3}, taken as 1000 kg/m^3)

s = specific gravity of sediment (taken as 2.65)

1.3 Predictive Equations

Engineers and geomorphologists have developed many equations for estimating sediment transport rates. In this paper, field data using Equation [1-1] are compared to estimates from four different predictive equations: the Meyer-Peter, Müller ,MPM; formula (Meyer-Peter and Müller 1948, Wong and Parker 2006), Rosgen's Pagosa reference curve (Rosgen 2006), Wilcock's Two Parameter Model (Wilcock 2001), and Bathurst's Phase 2 bedload transport equation (Bathurst 2007).

1.3.1 The Meyer-Peter, Müller Equation

$$q^*_s = 8(\tau^* - \tau^*_c)^{3/2} \quad \textbf{[1-2]}$$

where:

q*s = dimensionless bedload transport rate per unit width of streambed

τ* = dimensionless shear stress

τ*c = dimensionless critical shear stress (taken to be 0.04)

In order to find the dimensionless shear stress, τ*, the dimensional shear stress, τ, is found using

$$\tau = \gamma HS \quad \textbf{[1-3]}$$

where:

τ = sheer stress (FL^{-2})

γ = specific weight of water (FL^{-3})

H = depth (L)

S = slope (L/L)

This shear stress is non-dimensionalized for use in equation [1-2] by

$$\tau^* = \frac{\tau}{(s-1)\gamma D} \qquad \textbf{[1-4]}$$

where:

τ^* = dimensionless sheer stress

s = 2.65

γ = specific weight (FL^{-3})

d_{50} = particle size for which 50% of the material is finer (L)

For the purposes of comparing predicted to observed values, the q*s value from equation [1-2] is then redimensionalized to find the transport rate in L^3T^{-1}:

$$Q_S = \left(\frac{q_s^*}{(s-1)g\rho^{3/2}} \right) b \qquad \textbf{[1-5]}$$

where:

Q_s = bedload transport rate (L^3T^{-1})

q^*_s = dimensionless transport rate per unit width

s = 2.65

g = gravitational acceleration (LT^{-2})

ρ = density of water (ML^{-3})

b = streambed width (L)

1.3.2 Rosgen's Pagosa Reference Curve

David Rosgen's Pagosa Reference Curve (Rosgen 2006) is an empirical dimensionless transport equation derived from bedload measurements on three rivers. The rating curve relates bedload transport rates (made dimensionless by dividing all bedload rates by the bedload transport rate found at bankfull flow rates).and flowrate (made dimensionless by dividing all flow rates by the bankfull flow rate).

$$Q^*_S = -0.0113 + 1.0139(Q^*)^{2.1929} \quad \textbf{[1-6]}$$

where:

Q^*_s = dimensionless bedload transport rate

Q^* = dimensionless discharge

Like the Meyer-Peter, Müller formula, the final results are redimensionalized in order to compare to observed rates using the Qs value taken at bankfull conditions using the Qs value taken at bankfull conditions.

1.3.3 Wilcock's Two Parameter Model

This model is based on the Meyer-Peter, Müller equation, but has the advantage of being calibrated with observed data. In order to calibrate the Wilcock Model (Wilcock 2001), field observations are non-dimensionalized using the Meyer-Peter, Müller formula, then finding τ^* from τ. The τ^* value is plotted against a dimensionless transport variable w^*

$$w^* = \frac{(s-1)gq_s}{(\tau/\rho)^{3/2}} \quad \textbf{[1-7]}$$

where:

s = specific gravity of sediment (taken to be 2.65)

g = gravitational acceleration (LT^{-2})

τ = shear stress (FL^{-2})

ρ = density of water (ML^{-3} and taken to be 1000 kg/m^3)

By setting w^* to a reference value of 0.002, a t^*_r value is found. At this point, depending on the relationship between τ^* and t^*_r, one of two equations is used to find a dimensionless transport rate, q_s^*

$$q_S^* = 0.0025\left(\frac{\tau^*}{\tau_r^*}\right)^{14.2} \quad when \quad \tau^* \le \tau_r^* \quad \textbf{[1-8]}$$

or

$$q_S^* = 11.2\left[1. - 0.846\left(\frac{\tau_r^*}{\tau^*}\right)\right]^{4.5} \quad when \quad \tau^* > \tau_r^* \quad \textbf{[1-9]}$$

where:

q^*_s = dimensionless transport rate per unit width

τ^*_r = dimensionless shear stress, found where $w^* = 0.002$

As with the MPM formula, the results are redimensionalized for comparative purposes using

$$Q_s = \frac{q_S^*(\tau/\rho)^{1/2} b}{(s-1)g} \qquad \textbf{[1-10]}$$

where:

Q_s = bedload transport rate (L^3T^{-1})

q^*_s = dimensionless transport rate per unit width

1.3.4 Bathurst's Phase 2 Bedload Transport Equation

The Bathurst method (Bathurst 2007) considers bedload transport as supply-limited by a coarse armor layer (Phase 1), until a critical discharge, q_{c2}, is reached. When flows exceed the critical discharge, motion of armor layer particles is initiated; the Phase 2 equation [1-11] predicts bedload rates with

$$q_s = \alpha\rho(q - q_{c2}) \qquad \textbf{[1-11]}$$

where:

q_s = bedload transport per unit width (MT^{-1})

α = rate of bedload change as discharge changes

ρ = density of water (taken as 1000 kg/m^3)

q = stream discharge per unit width (L^2T^{-1})

q_{c2} = critical value of discharge per unit width for initiation of motion (L^2T^{-1})

The relationship gradient, α, is found using

$$\alpha = 29.2S^{1.5}\left(D_{50}/D_{50s}\right)^{-3.30} \quad \textbf{[1-12]}$$

where

S = slope (LL^{-1})

D_{50} = bed surface particle size for which 50% of the material is finer (L)

D_{50S} = bed sub-surface particle size for which 50% of the material is finer (L)

and the critical discharge, q_{c2}, for each site is calculated using

$$q_{c2} = 0.0513g^{1/2}\left(\frac{D_{50}}{\rho}\right)^{3/2} S^{-1/2} \quad \textbf{[1-13]}$$

where:

q_{c2} = critical discharge per unit width defining onset of Phase 2 (L^2T^{-1})

g = gravitational acceleration (LT^{-2})

D_{50} = particle diameter for which 50% of bed surface material is finer (L)

ρ = density of water (taken as 1000 kg/m^3)

S = slope (LL^{-1})

Values for total bedload transport rate are found in units of L^3T^{-1} for comparative purposes using

$$Q_s = \frac{q_s b}{\rho S} \quad \textbf{[1-14]}$$

where:

Q_s = total bedload transport rate (L^3T^{-1})

q_s = bedload transport per unit width (MT^{-1})

b = stream width (L)

ρ = density of water (taken as 1000 kg/m^3)

S = specific gravity of sediment (taken to be 2.65)

1.4 Comparative Results between Observed and Predicted Rates

Because each sample site had a different slope, depth, and other flow parameters, observed bedload data were stratified by site, and predicted bedload rates were calculated for individual sites. Figure 1-4 through Figure 1-6 show the sediment rating curves that were developed for each site based on observations and predictions.

Figure 1-4 through Figure 1-6 show different results for each site, which can be simplified by the following four observations: I) the predicted rates from the uncalibrated Meyer-Peter, Müller equation are consistently four or more orders of magnitude larger than observed rates, II) the calibrated Wilcock equation performed better than the uncalibrated MPM formula, but also differed from observed rates by three or more orders of magnitudes at Sites 1 and 2; III) the Bathurst equation predicted rates within a order of magnitude of observed rates at Sites 1 and 3, and within two orders at Sites 2; and IV) the Rosgen curve predictions were within an order of magnitude at Sites 2 and 3, and between one and five orders of magnitude at Site 1.

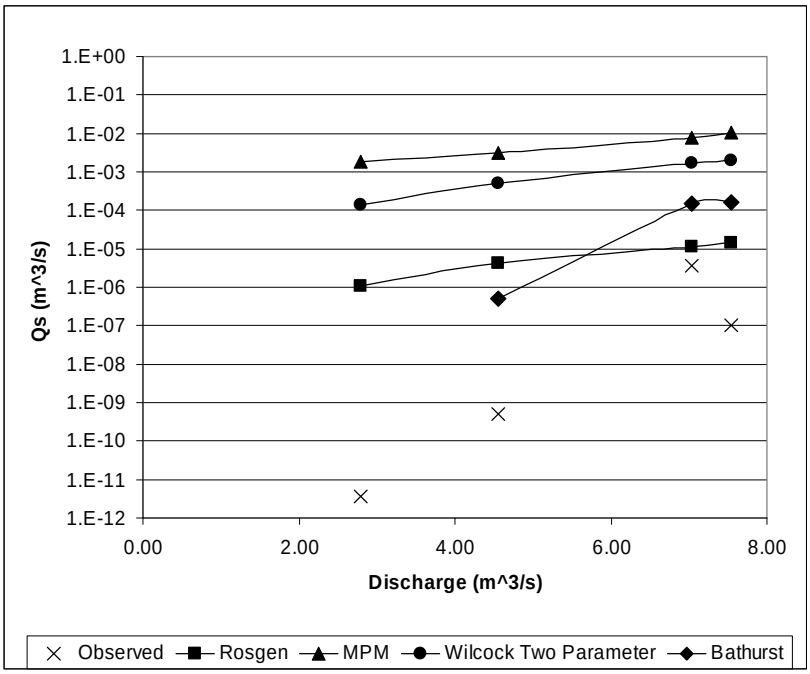

Figure 1-4. Predicted transport rates compared to observed rates at Site 1.

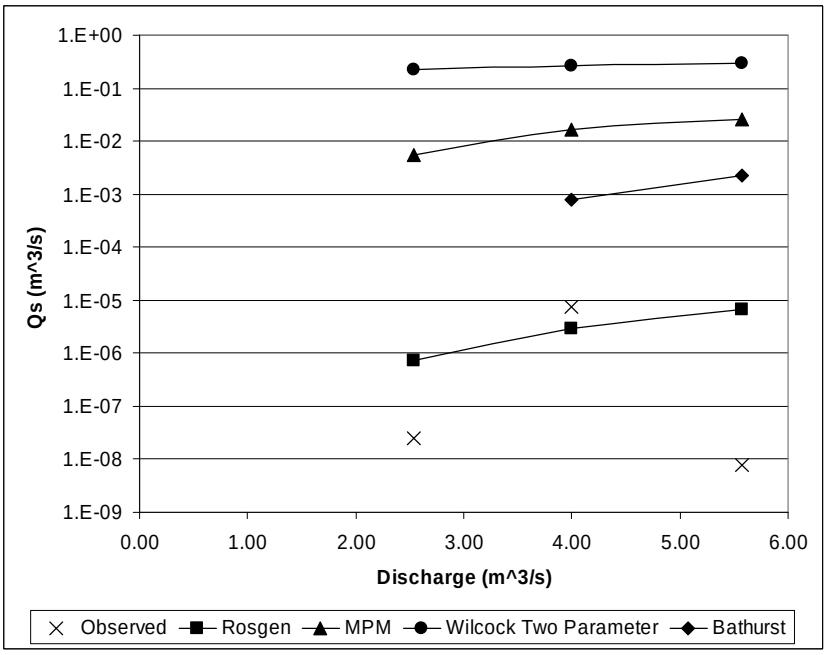

Figure 1-5. Predicted transport rates compared to observed rates at Site 2.

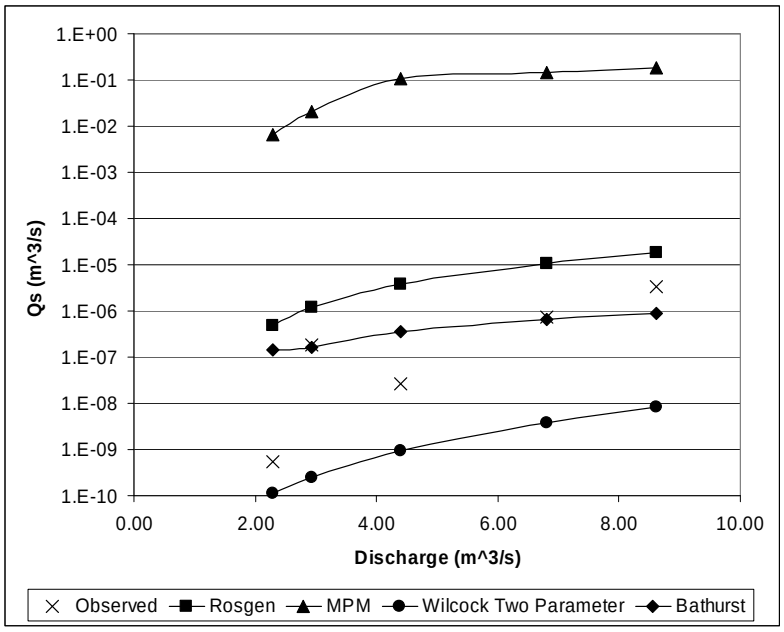

Figure 1-6. Predicted transport rates compared to observed rates at Site 3.

1.5 Ramifications of Discrepancies between Observed and Predicted Rates

Because sediment transport rates are a function of channel size, designing for different values of Q_s may result in different design channel dimensions. There are several methods for deriving channel sizes from sediment transport rate, but the general idea is to find a relationship between a transport equation and equations dealing with hydraulic geometries.

1.5.1 Use of Meyer-Peter, Müller to Find Channel Dimensions

The software SAM calculates stable channel dimensions from a predetermined discharge and bedload rate. The SAM method utilizes the MPM formula from 1948, the Limerinos equation for grain roughness, the Cowan equation for determining the total bed roughness coefficient, and Manning's equation for hydraulic calculations (Thomas et al 2002). In this study, the Wilcock method for calculating channel dimensions from

sediment transport rates was used. This differs slightly from the Sam method, by using the Wilcock form of Meyer-Peter, Müller and solving for shear stress, τ, by

$$\tau = \left[(s-1)\rho g D\right]\left[\tau_C^* + \left[\frac{Q_s}{8b\sqrt{(s-1)gD^3}}\right]^{2/3}\right] \quad \textbf{[1-15]}$$

Also uniform stream velocity, U, from Manning's equation is:

$$U = \frac{\sqrt{S}}{n} R^{2/3} \quad \textbf{[1-16]}$$

where:

S = stream slope (L/L)

R = hydraulic radius (L)

n = Manning's roughness coefficient

Design flow depth, h, can be found from the Manning equation and the continuity equation for a rectangular channel:

$$h = \frac{Q}{Ub} \quad \textbf{[1-17]}$$

where:

Q = discharge (L3T-1)

U = uniform stream velocity (LT-1)

b = stream width (L)

Hydraulic radius, R, is then found using

$$R = \frac{bh}{b + 2h} \qquad \textbf{[1-18]}$$

where:

b = stream width (L)

h = design depth (L)

Once the hydraulic radius is known, design slope, S, can be found using the shear stress, τ, from equation [1-15]:

$$S = \frac{\tau}{\gamma R} \qquad \textbf{[1-19]}$$

where:

τ = shear stress

γ = specific weight of water

R = hydraulic radius

Following this sequence of calculations iteratively, channel dimensions of depth, slope, and width can be determined. Because equations 1-14 through 1-18 are all interrelated, changing Qs values in equation 1-10, will change τ, S, U, h, and R in the other equations, and a different design channel will result.

1.5.2 Channel Dimensions for Hobble Creek Sites

The process outlined above was used to determine hypothetical "design" dimensions along Hobble Creek based on the observed and predicted transport rates for each site. Four different Q_s values were used at each site to find channel dimensions: the observed Q_s, and each of the four model's predicted Q_s values. The five resulting design cross sections (one derived from observed Qs rates and four derived from predicted rates) are compared to currently existing cross sections in Figures Figure 1-7 through Figure 1-9.

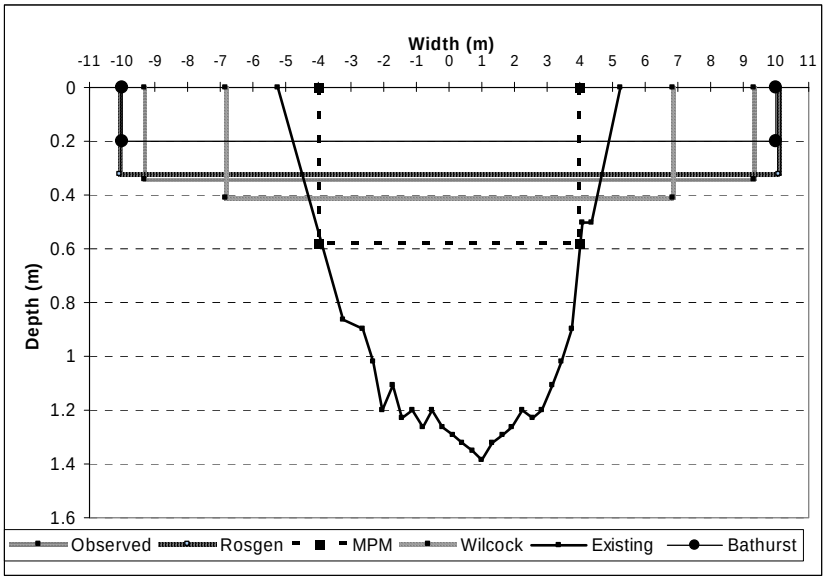

Figure 1-7. Design cross sections for Site 1, based on observed and each model's predicted Qs values at bankfull flow rates. Also included is the existing cross section.

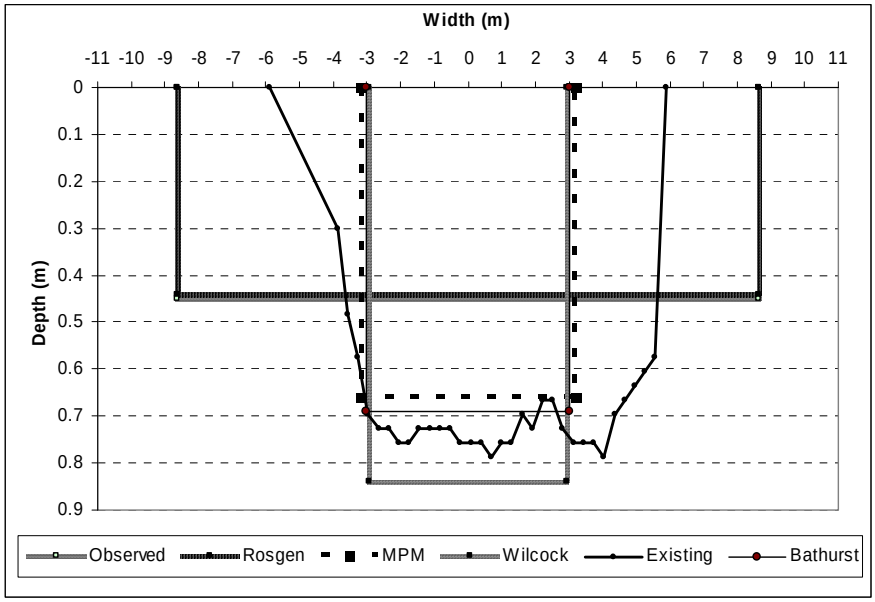

Figure 1-8. Design cross sections for Site 2, based on observed and each model's predicted Qs values at bankfull flow rates. Also included is the existing cross section.

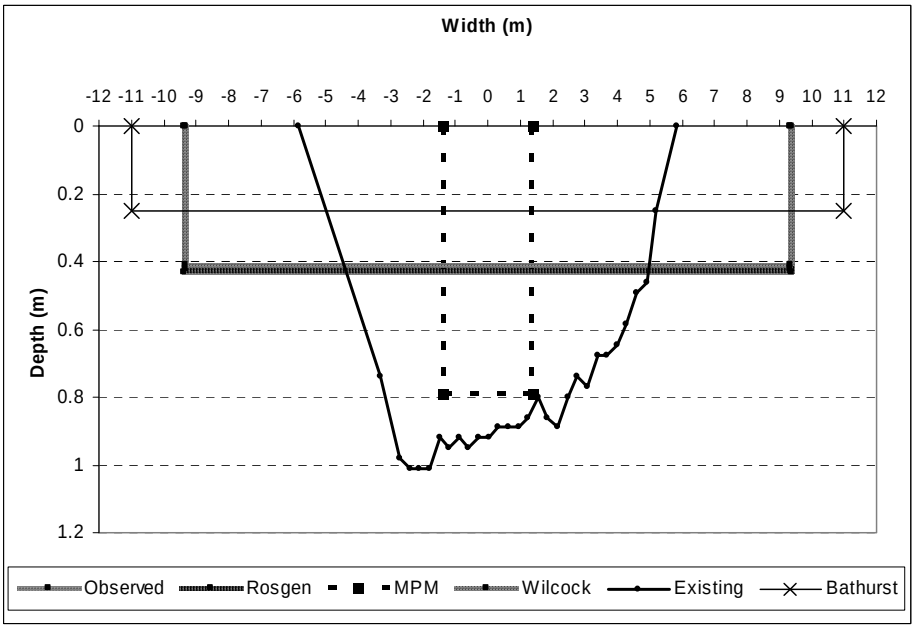

Figure 1-9. Design cross sections for Site 3, based on observed and each model's predicted Qs values at bankfull flow rates. Also included is the existing cross section.

1.5.3 Discussion on Channel Dimensions

Urbanization and flood control efforts extending over the past century since settlement of Utah Valley have considerably altered Hobble Creek's course, shape, and hydrologic regime. A discrepancy between the type of steam observed bedload values might naturally create and what now exists can only be expected. Two items of interest that are seen in the preceding figures are: 1) models that predict higher than observed bedload transport rates necessitate deeper, narrower channels than models that predict transport rates closer to observed values; and 2) the channel dimensions as they currently exist are narrower and deeper than needed by the bedload rate that actually occurs.

1.6 Conclusions

The objective of this study was to demonstrate the importance of field data in a stream restoration effort. Bedload and the variables that control it vary considerably between locations, and a predictive equation may not account for every possible controlling parameter. For example, the Bathurst equation accounts for a course armor layer that limits supply; this may significantly improve the predicted rate accuracy over non-calibrated, capacity limited equations, but there may be other factors besides the armor layer in limiting bedload on Hobble Creek

While these results can be applied specifically to the Hobble Creek restoration effort, they are also generally applicable to all restoration projects involving channel design and re-alignment. Although some sediment transport models may predict a transport rate close to that which actually occurs, uncalibrated models may mispredict rates by several orders of magnitude, resulting in an incorrect channel design. Better

even than a calibrated model, bedload transport rates obtained in the field, though expensive to obtain, are more reliable than any model, and less expensive than a project failure.

2 On Determining Rearing Habitat for Larval June Sucker

Chapter Abstract

The objective of this study is to provide insight on the current stream lake interface zone of Hobble Creek and Utah Lake and determine what attributes that interface may need to create a self-sustaining population of June sucker. A restoration project on Hobble Creek, Utah, USA aims to restore spawning habitat for the June sucker (*Chasmistes liorus*). With this goal in mind, the fate of larvae, in terms of adequate access to food and warm waters, becomes an important issue to be considered in the design phase of the project. June sucker and many other species depend on the transition zone between stream and lake, yet this interface area is a poorly understood facet of the limnological system. We divided the interface area in to four sample zones: open lake, sparse vegetation, dense vegetation, and the creek. We sampled for resource availability (zooplankton and benthic invertebrates), measured existing small fish densities, and determined temperature profiles in the lake zones over a 6 month period. Analyses of the zooplankton and benthos data indicate that zones differ from each other in regards to community composition and the open lake zone has the highest amounts of the most important taxa that larval June sucker depend on. Small fish are most abundant in the open lake, and temperatures are coolest in the dense vegetation zone. All these data combine to indicate that the ideal habitat for rearing larvae is in the open lake, but current flow patterns will prevent larvae from reaching that habitat. Conclusions are 1) that the

stream lake interface shows a progression of vegetation densities, temperatures, and communities as the system transitions from stream to lake; 2) that larval survival is dependant on their ability to find the warm, food rich waters of the open lake, and 3) that we see a need for better understanding of lake-stream interface areas in general.

2.1 Introduction and Hypotheses

The restoration project on Hobble Creek, Utah, USA aims to restore spawning habitat for the June sucker. With that objective in mind, the fate of larvae, in terms of adequate access to food and warm waters, becomes an important issue that project designers need to consider. Historically, June sucker spawned up all the major inflowing rivers in to Utah Lake, currently they are limited to spawning only in the Provo River. The goal of the restoration project is to create an additional self-sustaining population besides the population that currently uses the Provo River. June sucker recruitment failure on the Provo River has not been attributed to reproductive failure (Modde and Muirhead, 1994) but to larvae failing to make it to suitable rearing habitats. Due to channelization of the Provo, a long lake-influenced portion of the lower reach has very slow flows that result in larval starvation before they reach the food-rich habitat in the lake. Hobble Creek is currently similarly channelized, and ensuring that larvae will find adequate resources is paramount to the success of the project.

The lentic-lotic interface is a poorly understood facet of the freshwater ecosystem, and documentation in the literature is scanty at best. Complex variations of water chemistry, community, temperature, vegetation density, and sediment distribution exist in this area (MacKenzie and Kaster 2004, Turner and Rao 1990). Since June sucker and

many other fish species depend on the stream-lake interface, understanding the ecological forces at work within the interface zone will provide valuble insight to project planners on how to address the fate of larval survival.

June sucker larvae require warm, food rich waters (Belk, unpublished data) to maximize growth rates as early in life as possible. Because Hobble Creek has been channelized and rerouted from original pathways, it is unclear where suitable habitat is, and whether or not larval June suckers will make it to that habitat before starvation occurs. The "ideal area" will likely depend on several variables, which include food density, cover habitat, and temperature (Crowder 1982). Access to resource-dense zones is crucial to larval survival and open lake areas are most likely to contain highest amounts of plankton, the primary food source for the June sucker (Belk, unpublished data). As warmer temperatures are associated with higher growth rates, survival rates may be optimized by ensuring that young June sucker arrive in warm shallow areas in the shortest time possible after hatching. Areas with higher concentrations of macrophyte density would be expected to have lower temperatures due to proximity with cooler creek water and effects of shading.

The objective of this study is to provide insight on the current stream lake interface zone of Hobble Creek and Utah Lake, and determine what attributes that interface may need to create a self-sustaining population of June sucker.

2.2 Methods

To determine habitat suitability, the stream-lake interface was divided into three zones: 1) "dense" emergent vegetation (> 20 stems/m^2), 2) "sparse" emergent vegetation

(0-15 stems/m^2), and 3) "open lake" with no emergent vegetation. The flowing channel of Hobble Creek was a fourth zone ("creek") about 1 km upstream from the confluence of the lake. Three evenly spaced transects extended perpendicularly from the shore through each vegetation zone of the stream-lake interface (Figure 2-1).

We obtained resource availability samples from nine sites in each zone of the stream-lake interface. Since the width of the sparse zone differed between the three transects, samples were taken at ¼, ½, and ¾ of that zone's width. The distance between sites in the dense and open lake zones was 50, 100, and 150 meters from the shoreward border. We also collected samples at three sites located ¼, ½, and ¾ across the width of Hobble Creek at three different locations along the creek.

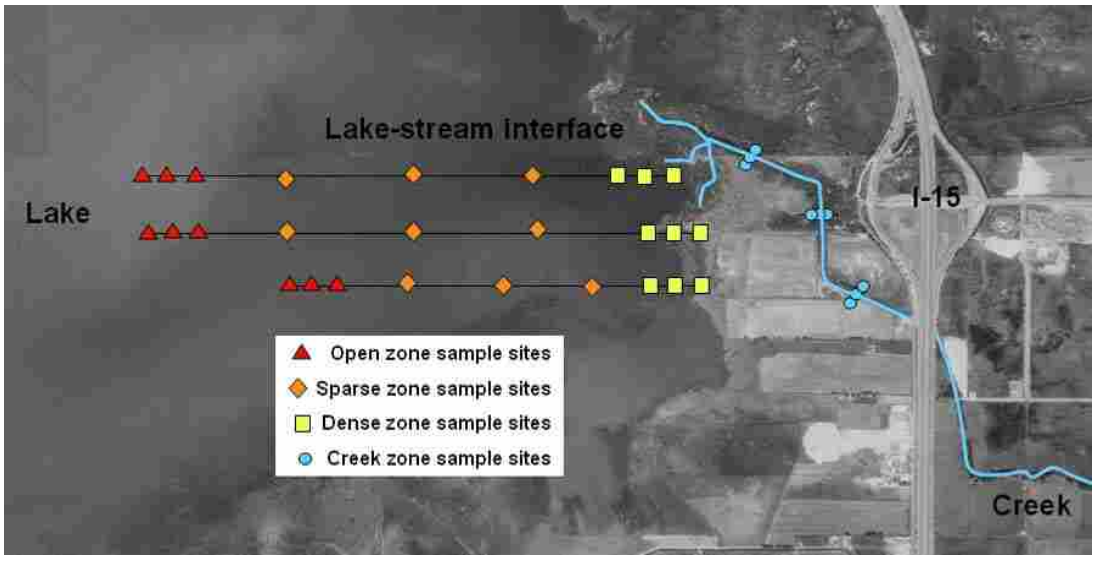

Figure 2-1. Utah Lake, Hobble Creek, and the stream-lake interface showing sampling sites in each of the four zones.

The locations within the creek were randomly chosen from the upper, middle, and lower sections of the creek by dividing the length of each section into evenly spaced 10-

meter segments; then we randomly chose one segment out of each section, and took our samples in that segment. All sites were sampled once in June and again in August of 2006. A handheld GPS unit was used to relocate the same sites in both months

We collected both zooplankton and benthic invertebrate samples at each site in both months to quantify differences in June sucker food availability between zones. Zooplankton were collected by drawing a plankton net (64 μm mesh) from the bottom through the water column. Zooplankton density (number/liter) was based on the distance of a tow multiplied by the area of the net opening. A clear Plexiglas tube (6.5 cm diameter) was inserted vertically through the water column, capped on both ends, and poured through a 64 μm mesh to estimate zooplankton densities in dense vegetation. All zooplankton samples were placed in 500 ml Whirlpaks and preserved in 95% ethanol.

A clear plexiglass core (5 cm diameter) was used to quantify differences between sites in the density of benthic invertebrates (numbers/m^2). The same amount of sediment was collected from each sample because the core was fitted with a collar 2.5 cm from the opening. The contents of each core were preserved in 95% ethanol.

In the laboratory, five sub-samples (2 ml) were removed and individually enumerated using a strip-count technique under a compound microscope (100x magnification). Each sample was placed in a 100 ml beaker of distilled water and shaken before extracting a subsample of 2 ml. Total sample density was estimated as the sum of the five sub-samples multiplied by ten.

Benthic samples were rinsed through a 64 μm sieve and poured into a Plexiglas tray sectioned into 24 quadrants (36 cm^2 each). Six quadrants were randomly chosen and the macroinvertebrates removed for enumeration under a compound microscope (100x

magnification). The total sample density was estimated as the sum of the six sub-samples multiplied by four. Zooplankton and benthos samples were statistically analyzed to differentiate between categories of data and location. We used ANOSIM to generate Non-Metric Multi-Dimensional Scaling (NMDS) plots for each dataset comparison, then performed additional analyses with SIMPER to gain insight on what taxa created distinctions between sample groups.

The density of small fish from a variety of species was estimated in each zone using minnow traps. Four traps were placed simultaneously at a randomly selected sample site in each zone. Minnow traps were also placed at one randomly selected creek sample site. After 24 hrs the fish in each trap were counted and identified to genus or species. Fish data were analyzed using ANOVA to determine significance of differences between zones. Water temperature was also recorded (StowAway® thermographs, Onset Computer Corporation) every hour in each zone from June to October of 2006.

2.3 Zooplankton Results

Zooplankton community compositions varied considerably ($p = 0.009$) between the two sample dates (Figure 2-5) and therefore were separated into June and August categories for comparison between zones. Zooplankton samples taken out of the creek were so different from the three lake zones that they caused the lake zones to appear to be similar in the NMDS plot (see Figure 2-6). Once the creek zone data were removed, as seen in Figure 2-7, the difference between lake zones became more apparent. SIMPER analyses for the June data attribute the dissimilarity between dense and sparse zones to ostracods being 3 times more abundant in the sparse vegetation than they were in the

dense zone. Dissimilarity between dense and open zones is attributed to double the amount of copepod nauplii in the sparse than were in the dense zone, and dissimilarity between open and sparse zones is attributed to 1.5 times as many nauplii in the open lake than in the sparse vegetation.

Of primary interest to larval June sucker diet are rotifers, copepods, and cladocerans; all been found in gut analyses of larval June sucker (Gonzalez 2004). In June, the zone with the highest average abundance was open lake with approximately 450 rotifers per liter and 280 copepods per liter. The sparse zone had the highest number of cladocerans, with 460 organisms per liter sampled (see Figure 2-2, Figure 2-3, and Figure 2-4). The Type III F value for rotifers is 6.51, for copepods it is 11.83, and for cladocerans the F value is 2.74

The total absence of plankton in the creek during the August sampling time created the same scenario as was observed in the June samples, so again the creek data were removed in the NMDS plots to more clearly show that the lake samples were in fact dissimilar from each other. Results of August sample data are shown with and without data from the Creek zone in Figure 2-8 and Figure 2-9 respectively. SIMPER analyses on the August data attribute the dissimilarity between dense and sparse zones to cladocerans in the sparse vegetation being 1.5 times as abundant as they are in the dense vegetation. Dissimilarity between dense vegetation and open lake zones is attributed to the open lake having twice as many rotifers, copepods, cladocerans, and copepod nauplii as the dense vegetation had. Dissimilarity between open lake and sparse vegetation is attributed to twice the average abundance of rotifers and cladocerans in the open than were found in the sparse vegetation.

As was the case in June, August sample data showed that the zone with highest plankton availability was in the open lake zone. Rotifers, copepods, and cladocerans were found in abundances of 1280, 450, and 70 organisms per liter, respectively (see Figure 2-2, Figure 2-3, and Figure 2-4). The Type III F value for Rotifers is 6.51, for Copepods it is 11.83, and for Cladocerans it is 2.74.

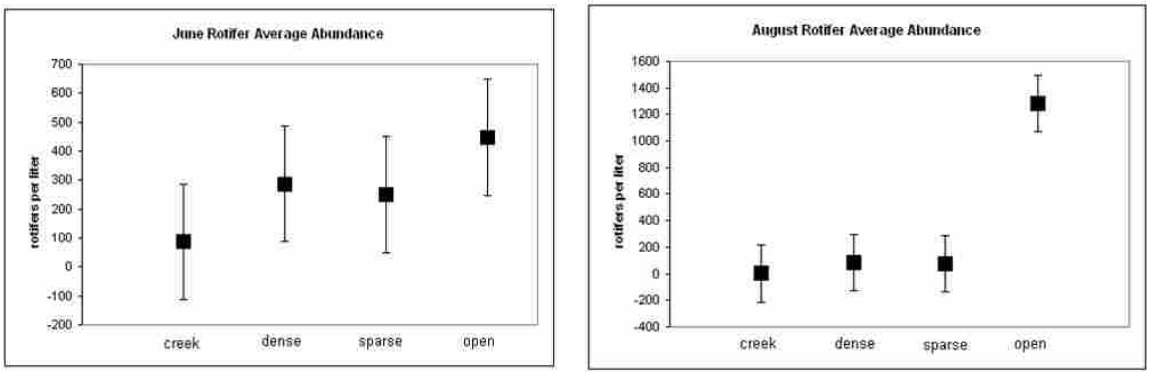

Figure 2-2. Rotifer average abundance by zone.

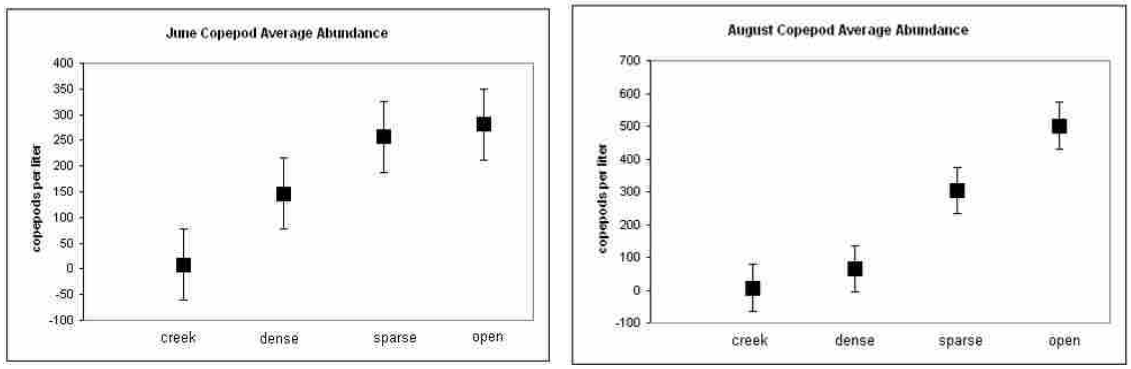

Figure 2-3. Copepod average abundance by zone.

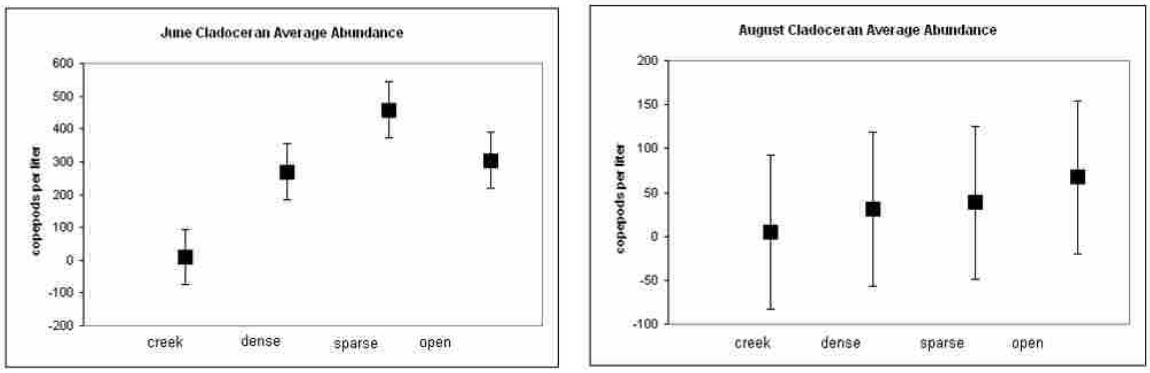

Figure 2-4. Cladoceran average abundance by zone.

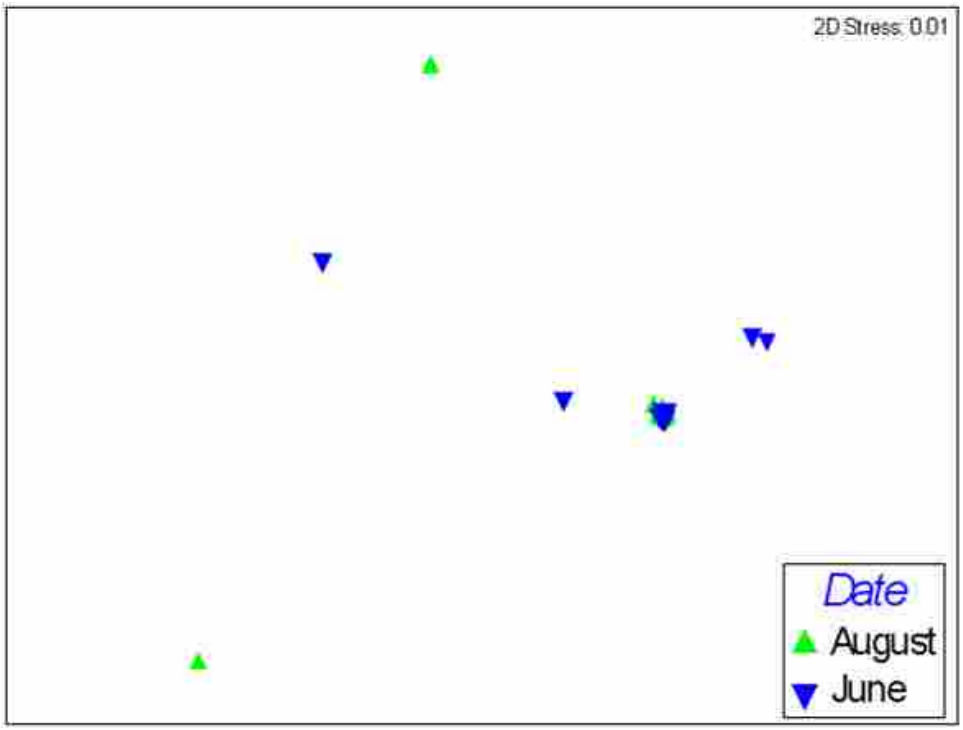

Figure 2-5. Non-Metric Multidimensional Scaling showing the difference in the community composition of zooplankton between June and August, 2006.

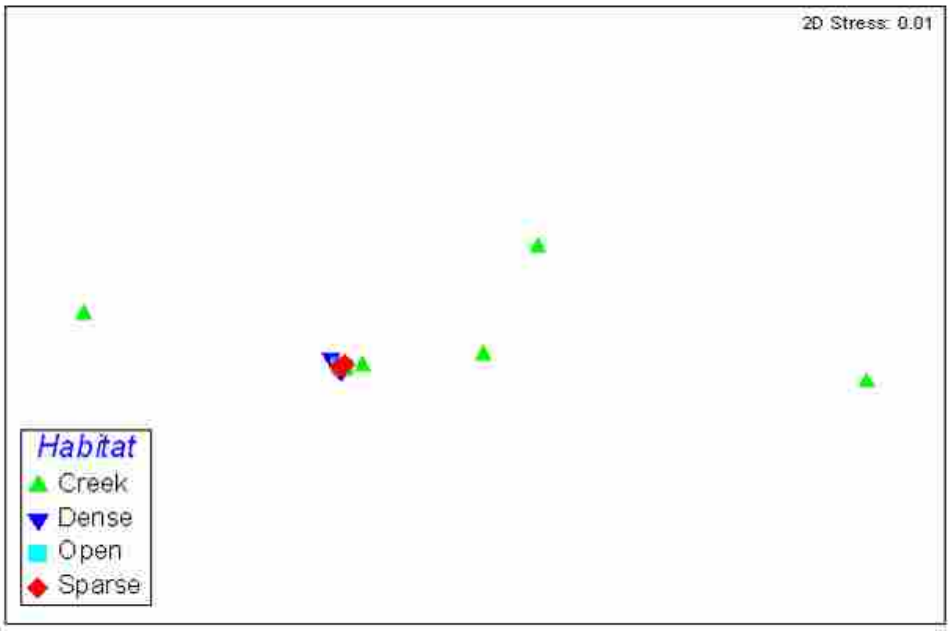

Figure 2-6. Non-Metric Multidimensional Scaling showing the difference in community compositions between the four sample zones during June, 2006.

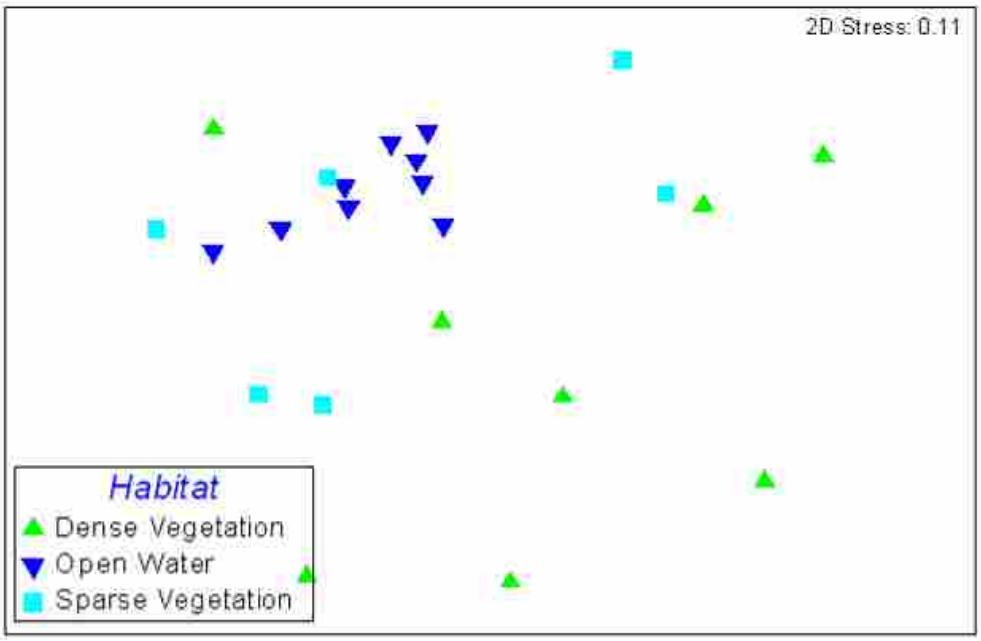

Figure 2-7. Non-Metric Multidimensional Scaling showing the difference in the three lake zones during June, 2006. With the creek samples removed, the difference between the three lake zones is more apparent.

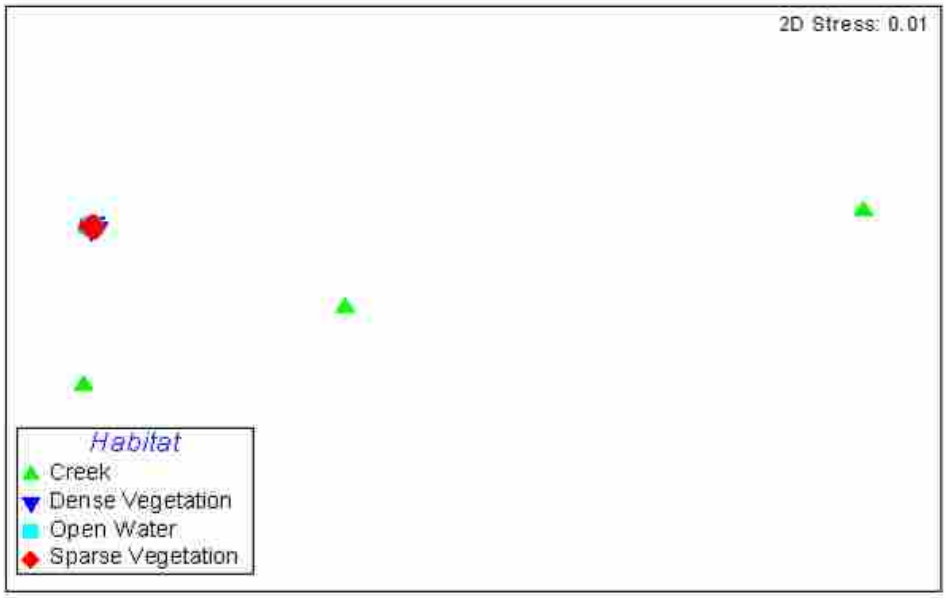

Figure 2-8. Non-Metric Multidimensional Scaling showing the difference in the four sample zones during August, 2006. Creek data create the illusion that the lake zones are identical.

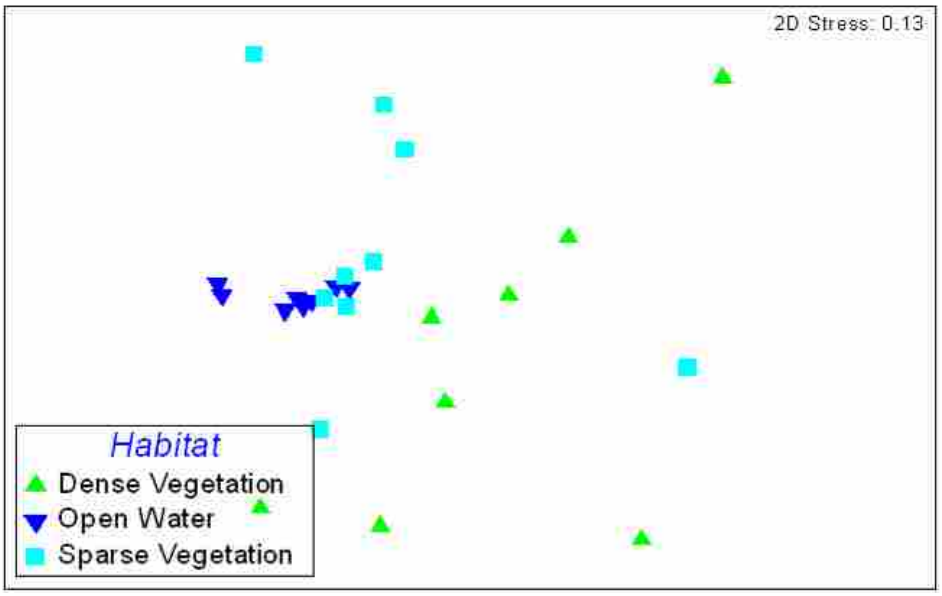

Figure 2-9. Non-Metric Multidimensional Scaling showing the difference in the three lake zones during August, 2006. With the creek samples removed, the difference between lake zones is more apparent.

2.4 Benthos Results

Benthic invertebrate community compositions were found to vary significantly ($p = 0.001$) between the June and August sampling times, as seen in Figure 2-10. For this reason, the June and August samples were then analyzed separately.

June benthos sample analysis shows that all four zones were statistically different ($p \leq 0.001$) from each other (see Figure 2-11), with the creek zone being the area with highest amount of organisms. Samples taken in August also showed the four zones to vary significantly ($p \leq 0.001$), with the open lake zone and the creek zone having higher counts than the other two zones (see Figure 2-12).

SIMPER analyses on June benthos data indicate that the dissimilarity between the creek and the open lake is attributed to 25 times as many harpactacoids, 6 times as many nematodes, 8 times as many ostracods, 3 times as many chironomids, and twice the average abundance of oligochaetes in the creek as were found in the open lake. Dissimilarity between the creek and the sparse vegetation is attributed to 6 times the average abundance of ostracods, 5 times as many amphipods, and 2 times the average abundance of chironomids. Dissimilarity between the creek and dense vegetation occurred due to 6 times the average abundance of nematodes, 10 times the average abundance of harpactacoids, twice as many oligochaetes, and 8 times as many ostracods in the creek than were found in the dense vegetation. Dissimilarity between the dense vegetation and open lake was attributed to 4 times the nematodes, twice the ostracods, and twice the chironomids in the dense vegetation as the open lake had. Sparse and dense vegetation zones dissimilarity was due to 4 times the nematodes, 3 times the chironomids, and 4 times the harpactacoids having been observed in the sparse zone than

were observed in the dense zone. Dissimilarity between open lake and sparse vegetation is due to 10 times the average abundance of harpactacoids and twice the number of ostracods in the open lake as was in the sparse vegetation.

Benthos samples in June from sparse and creek zones have the highest population densities, and all four zones are significantly different ($p \leq 0.001$). Benthos samples in August from open and creek zones have the highest population densities, and all four zones are significantly different.

SIMPER analyses on the August benthos data indicate that dissimilarity between the creek and dense vegetation is caused by the creek having 3 times as many oligochaetes, 3 times as many nematodes, and 7 times as many chironomids as the dense vegetation had, but there being 3 times as many ostracods in the dense vegetation than in the creek. Dissimilarity between the creek and sparse vegetation is attributed to the creek having 3 times as many oligochaetes and 7 times as many chironomids as were observed in the sparse vegetation. The dissimilarity between the creek zone and the open lake is attributed to the creek having twice as many oligochaetes and 3 times as many chironomids as were in the open lake. Dissimilarity between dense vegetation and open lake is due to 6 times as many nematodes in the open lake than in the dense; and dissimilarity between dense and sparse vegetation is due to there being twice as many ostracods in the dense as in the sparse zone. Dissimilarity between the open lake and the sparse vegetation is attributed to nematodes being twice as abundant on average in the open lake as they are in the sparse vegetation.

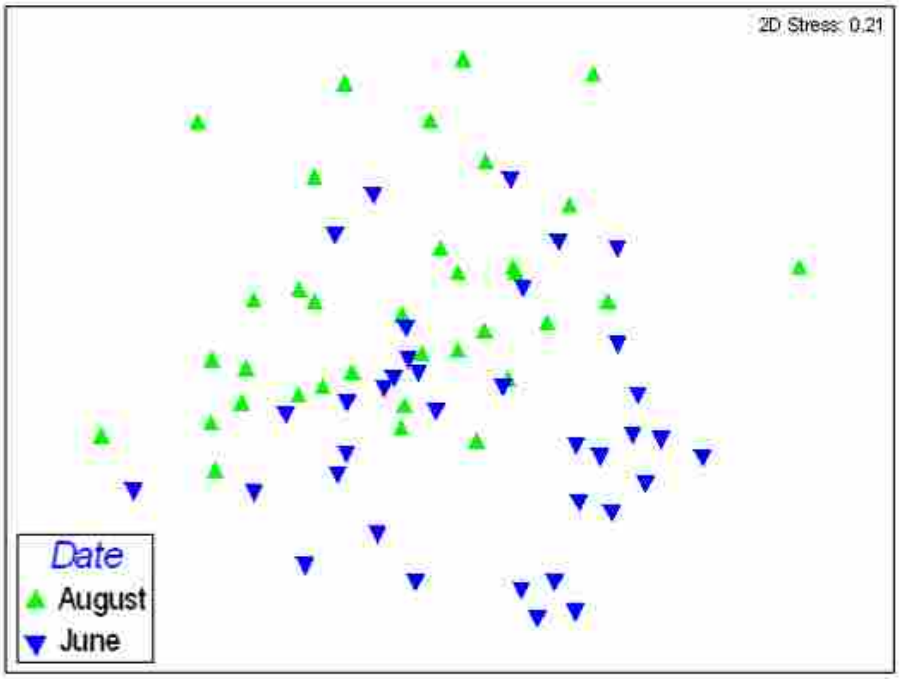

Figure 2-10. Non-Metric Multidimensional Scaling showing the difference in community composition of benthic invertebrates between June and August samples.

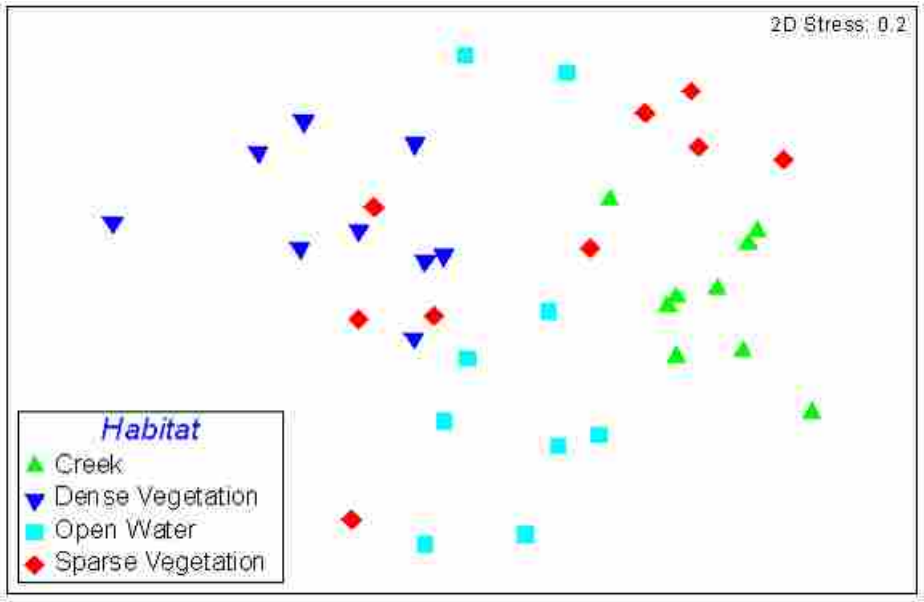

Figure 2-11. Non-Metric Multidimensional Scaling showing differences in the community composition of benthic invertebrates between zones of the stream-lake interface during June, 2006.

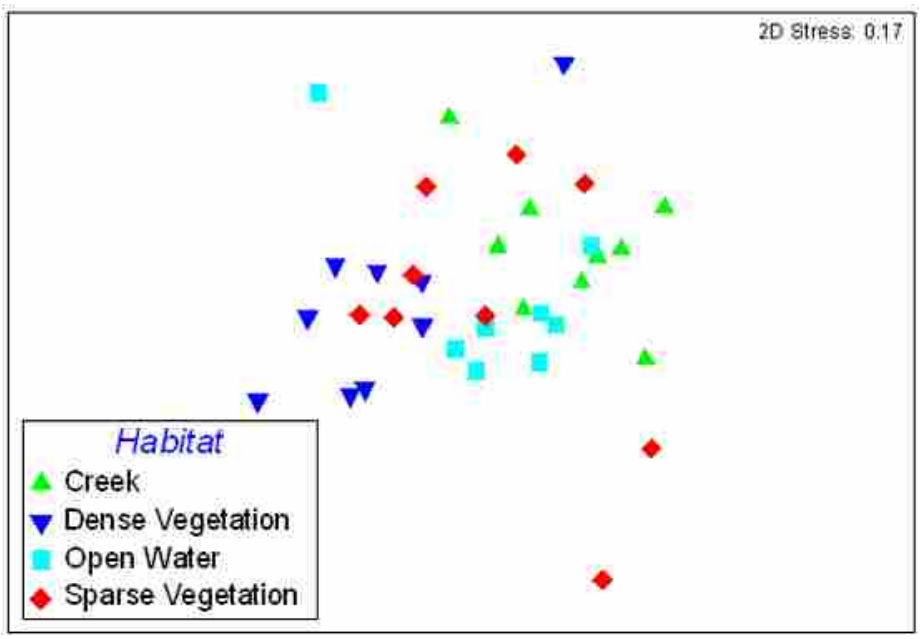

Figure 2-12. Non-Metric Multidimensional Scaling showing differences in the community composition of benthic invertebrates between zones of the stream-lake interface during August, 2006.

2.5 Minnow Trap Results

Small fish density data in the Hobble Creek – Utah Lake interface area were plotted for each zone. One of the traps in the dense zone was very near the surface due to shallow conditions, and several hundred western mosquitofish (*Gambusia affinis*) were found at the end of the 24 hour sample period. Mosquitofish are not a good model of larval June sucker; they are live bearing, consistently small bodied, and are surface feeders (FishBase 2007); consequently, we removed the mosquitofish data and plotted the average abundances for each zone. The dominant species found were Fathead minnows (*Pimephales promelas*) which feed on zooplankton like the June sucker (Page 1991). Fathead minnows were relatively evenly distributed throughout the open zone with specimens being found at all six sites in that zone, at an average density of 4.6 individuals

per trap (see Figure 2-13). The difference between the open and other zones is significant (Type III F value = 5.71).

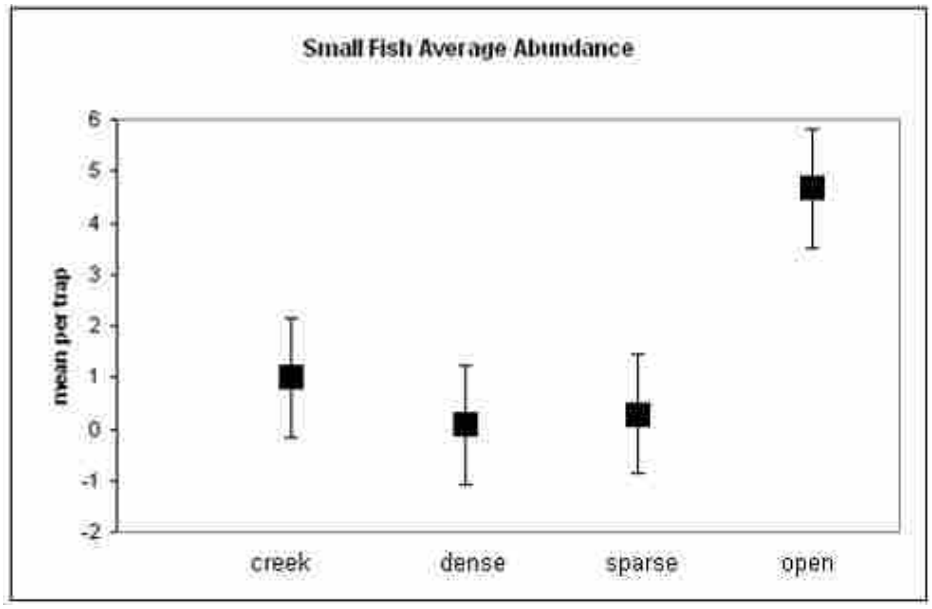

Figure 2-13. Small fish abundance in the four sample zones.

2.6 Temperature Probe Results

Temperature probes placed in the lake provide data on how large of an area the cool creek water extends into the lake and what the temperature difference is between the creek, lake and intermediate areas. Mean temperatures from each of the three lake zones was found, and the Dense zone, which is located nearest to both the shoreline and the mouth of the creek, was on average 3º C cooler than the other lake zones (see Figure 2-14).

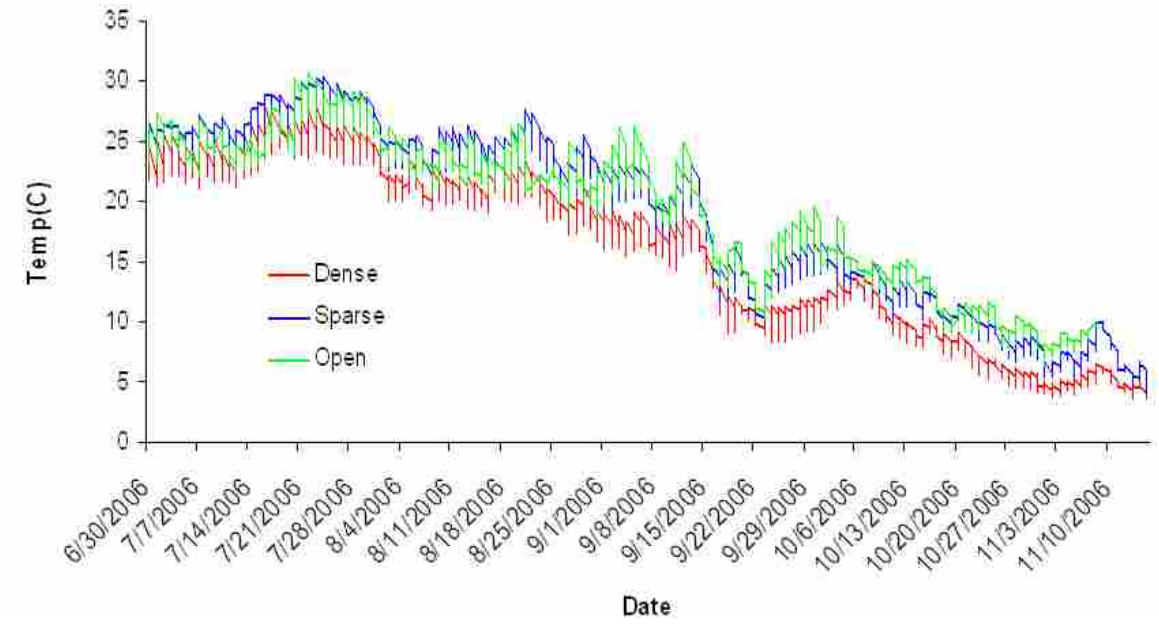

Figure 2-14. Temperature data from three lake zones.

2.7 Discussion

Data from zooplankton samples in June show that the four zones compared were all different from each other, with the creek being nearly void of plankton. Of the three lake zones, the open lake had highest population densities. Results from August zooplankton samples tell a similar story, with no plankton found in the creek and the open lake having significantly more than the other zones. Additionally, the SIMPER analyses on rotifers, copepods, and cladocerans show that vegetation-free areas in the lake are clearly where larval June sucker will find the most food.

Benthos data tell a slightly different story from the zooplankton data in terms of overall organisms per zone. Benthic invertebrates in both sample months were most dense in the creek zone, with sparse and open coming in second highest in June and August respectively. Although adult sucker utilize benthic invertebrates for food, larvae are not able to utilize those resources, which means that perhaps an adult could survive

for a time in the creek, but larvae cannot. Consequently, the most beneficial habitat, in terms of food resource availability, is open lake.

Small fish were found in highest numbers in the same zone as where highest food densities occur: the open lake. This indicates that larval June sucker will likely follow a similar trend, relying on numbers to overcome effects of predation in the open areas where refuge is absent, but food and warmth are plentiful.

Temperature gradients in the stream – lake interface of Hobble Creek and Utah Lake are clearly associated with vegetation density. Dense vegetation is again the least hospitable habitat for larvae, as temperatures were on average 3˚ C cooler than in the other two lake zones.

2.8 Conclusions

Several conclusions can be drawn from this investigation. One is that the stream-lake interface shows a progression of conditions that are affected by vegetation density as it changes from very dense vegetation to open lake habitat as the transition from lotic to lentic ecosystem occurs. We found distinct vegetation bands in the interface between Hobble Creek and Utah Lake, with correspondingly distinct communities in terms of zooplankton, benthic invertebrates, and small fish abundances.

In terms of suitability for the June sucker, it is clear that larval survival is dependant on their ability to find the warm, food rich waters of the open lake. This is unlikely to occur under present conditions (see Appendix F). Restoration designers need to ensure that their design includes an area of sufficiently deep water (> 2 m) that will inhibit vegetal growth, and provide a pathway from the creek out into the main body of

the lake. If this deeply dredged out zone is adjacent to shallower, vegetated zones, adequate refugia will be available to deter predation.

Lastly, we see a need for better understanding of lake-stream interface areas in general. These interface zones have complex dynamics that affect nutrient gradients, resource availability, temperatures and other factors crucial to the ecology of the system. While ecological principles may be well understood in lakes and streams individually, there is a paucity of data on the transition between the two. As designers proceed with restoration projects around this interface zone, acquisition of real data for that particular zone will be invaluable.

References

Bathurst, J.C. (2007). "Effect of course surface layer on bed-load transport." *J. Hydraul. Eng.*, 133(11), 1192-1205.

Bunte, K.; Swingle, K.W.; Abt, S.R. (2007)."Guidelines for using bedload traps in coarse-bedded mountain streams: construction, installation, operation, and sample processing." Gen. Tech. Rep. RMRS-GTR-191. Fort Collins, CO: U.S. Department of Agriculture, Forest Service, Rocky Mountain Research Station. 91 p.

Belk, M. Department of Biology, 401 WIDB. Brigham Young University, Provo UT 84602

Crowder, L. B., and Cooper, W. E. (1982). "Habitat Structural Complexity and the Interaction Between Bluegills and Their Prey." *Ecology,* 63(6), 1802-1813.

Doyle, M.W., Shields, D., Boyd, K.F., Skidmore, P.B., Dominick, D. (2007). "Channel-forming discharge selection in river restoration design." *J. Hydraul Eng.*, 133(7), 831-837.

"Gambusia affinis" FishBase. Ed. R. Froese and D. Pauly. November 2007 version. N.p.: FishBase, 2006.

Gonzales, David. Master's Thesis, BYU, 2004.

Mackenzie, R.A. and Kaster, J.L. (2004) "Temporal and spatial patterns of insect emergence in a Lake Michigan coastal wetland." *Wetlands*, 24(3), 688-700.

Meyer-Peter, E., and Müller, R. (1948). "Formula for bed-load transport." *Proc,. 2nd Meeting Int. Association for Hydraulic Structures Research*, Stockholm, 39-64.

Page, L. M. and Brooks M. B. (1991), *Freshwater Fishes*, p. 129-130, Houghton Mifflin, New York, NY.

Rosgen, D. (2006). *Watershed Assessment of River Stability and Sediment Supply*. Wildland Hydrology, Pagosa Springs CO.

Thomas, W.A., Copeland, R.R., and McComas, D.N. (2002) *User's manual for SAM hydraulic design package for channels*. Coastal and Hydraulics Laboratory, Vicksburg Miss.

Turner, R.A. and Y.S. Rao. (1990). "Relationships between wetland fragmentation and recent hydrologic changes on a deltaic coast." *Estuaries*, 13(3), 272-281.

Wilcock, P. R. (2001). "Toward a practical method for estimating sediment-transport rates in gravel-bed rivers." *Earth Surf.Process. and Landforms*, 26(13), 1335-1408.

Wong, M. and Parker, G. (2006). "Reanalysis and correction of bed-load relation of Meyer-Peter and Müller using their own database." *J.Hydraul. Eng.*, 132(11), 1132-1168.

Appendix A Bedload Data

Traps

Three types of traps were used to collect bedload data on Hobble Creek. Due to unwadeable conditions at the outset of our sampling period, traditional Bunte-Abt traps could not be used. For this reason the "Stanley" version of the Bunte-Abt traps was used for many of the samples taken early on. Starting on the 25 of May 2006 the flows had subsided to the point where wading and setting the Bunte-Abt traps became possible. In the most downstream sites (near I-15 and further downstream) fines represented a significant portion of the sediment, so a handheld Helley-Smith sampler with a 6" opening was used. The Helley-Smith sampler has a net with a mesh size of 0.25 mm, so sand and silt was retained and part of those samples. Data from sample sites where only a few (i.e. less than three) samples were taken were not included for analyses in the study above.

Summary Table

Table A-1 shows a summary of all the bedload data taken during May and June of 2006. This table includes not only bedload data such as location and mass obtained, but also data about each sample site, such as slope, surface particle sizes, and average depth. Since data from only three sample sites were used in the study discussed in Chapter 1

above, Figure A-1 has been included to show the relative locations of all sample sites were bedload measurements were taken.

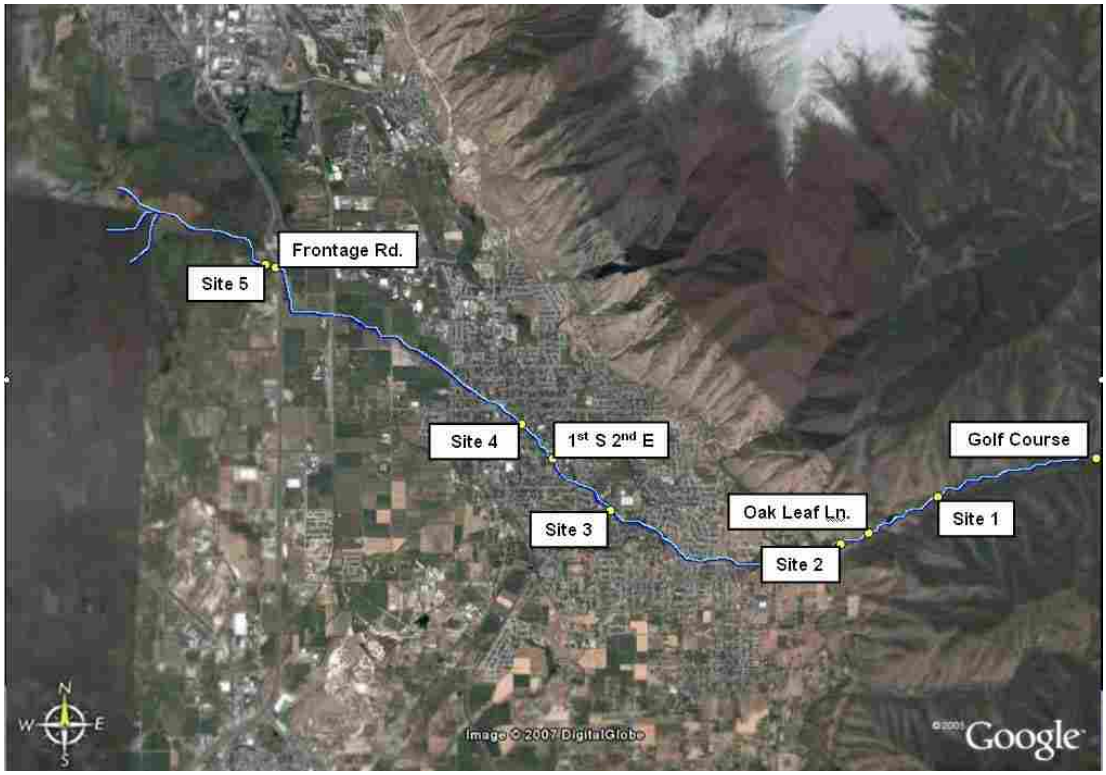

Figure A-1. Aerial view of Hobble Creek showing all sample sites.

Following Table A-1, Figure A-2 through Figure A-12 show the lateral variation of bedload transport within sites from day to day. The unit width discharge at each bedload trap is also included. Notice that higher transport rates do not necessarily coincide with higher unit discharge rates. Particle size distributions for each bedload sample obtained at a site on a single date are included as well.

Table A-1. Bedload summary table for bedload sampling period of spring 2006 on Hobble Creek.

Location	date	discharge (cfs)	sample weight (g)	sample time (min)	bed width (ft)	Sampling Device	Sampler Width (ft)	# of samples	slope (ft/ft)	D65 (mm) riffle-pool	Ave. Depth (ft)
Golf Course	3-May	473.1	14830.1	5	16	Stanley	1	6	0.01	95	2.3
Oak Leaf	27-Apr	389.0	2270.5	2	20	HS	0.5	10	0.017	100	3.30
Oak Leaf	15-May	129.5	23.4	5	23	Stanley	1	14	0.017	100	2.29
Site 1	11-May	266.1	29.2	5	19	Stanley	1	7	0.007	80	2.38
Site 1	18-May	248.4	1724.7	5	18	Stanley	1	11	0.007	80	2.20
Site 1	27-May	160.9	0.5	10	16	Stanley	1	10	0.007	80	1.82
Site 1	31-May	98.7	0.01	60	18	B/A	1	5	0.007	80	1.61
Site 2	23-May	196.7	4	5	23	Stanley	1	15	0.015	98	1.55
Site 2	25-May	140.9	1795.7	5	23	B/A	1	7	0.015	98	1.34
Site 2	31-May	89.5	73.94	60	23	B/A	1	7	0.015	98	1.01
Site 3	17-May	304.5	1726.4	5	22	Stanley	1	14	0.028	90	2.06
Site 3	19-May	240.7	366	5	22	Stanley	1	14	0.028	90	1.85
Site 3	24-May	155.2	12.55	5	22	Stanley	1	13	0.028	90	1.53
Site 3	30-May	103.2	626.76	60	22	B/A	1	8	0.028	90	0.75
Site 3	1-Jun	80.6	1.3	60	16	B/A	1	4	0.028	90	0.58
1st S 2nd E	27-Apr	457.0	6333.3	2	24	HS	0.5	4	0.007	100	3.20
Site 4	26-May	134.9	4.43	60	18	Stanley	1	4	0.02	95	1.95
Site 4	1-Jun	76.3	0.01	60	18	B/A	1	4	0.02	95	1.48
Frontage Rd.	27-Apr	512.0	5139.3	2	22	HS	0.5	11	0.001	18	5.30
Frontage Rd.	2-May	461.7	991	2	24	HS	0.5	11	0.001	18	5.22
Site 5	30-May	93.6	0.01	15	20	HS	0.5	4	0.001	n/a	3.60

Details

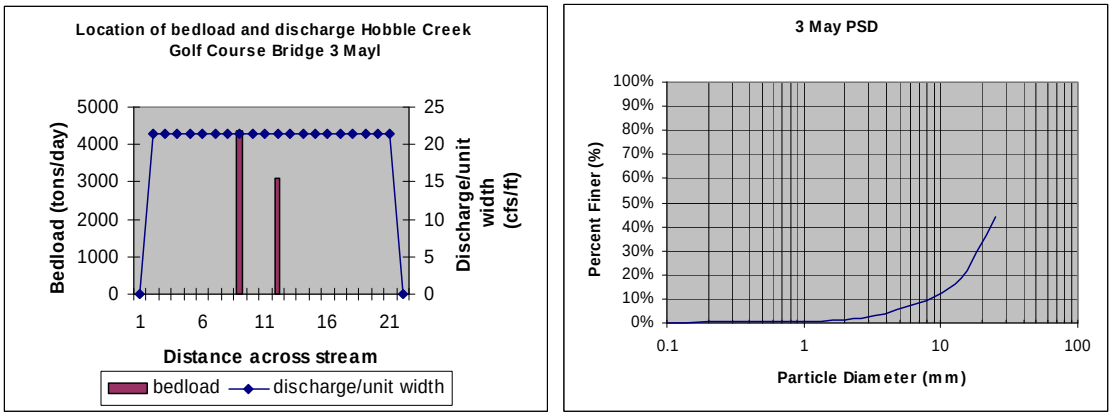

Figure A-2. Location of bedload movement, associated discharge, and particle size distribution for bedload sample taken at Golf Course bridge, 3 May, 2006.

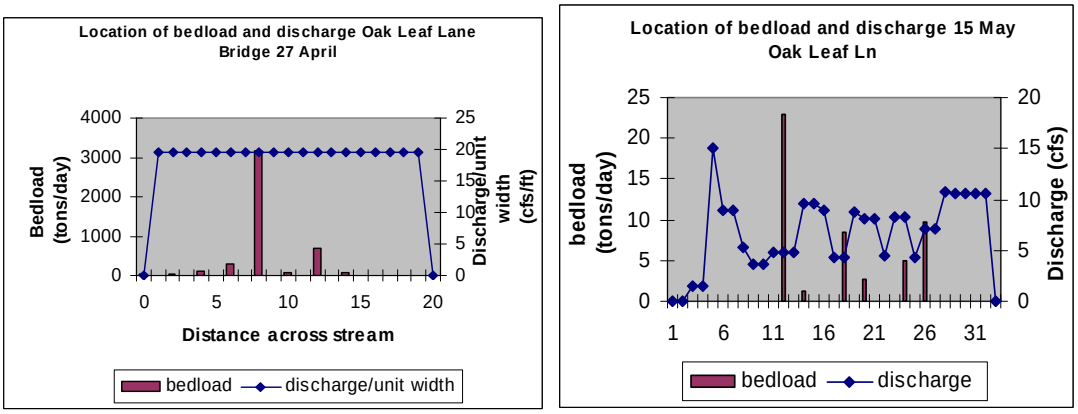

Figure A-3. Location of bedload movement, associate discharge for bedload sample taken at Oak Leaf Ln on 27 April, 2006. The discharge on 27 April was measured using the "sunkist method", and assumed here to be uniformly distributed across the width of the stream.

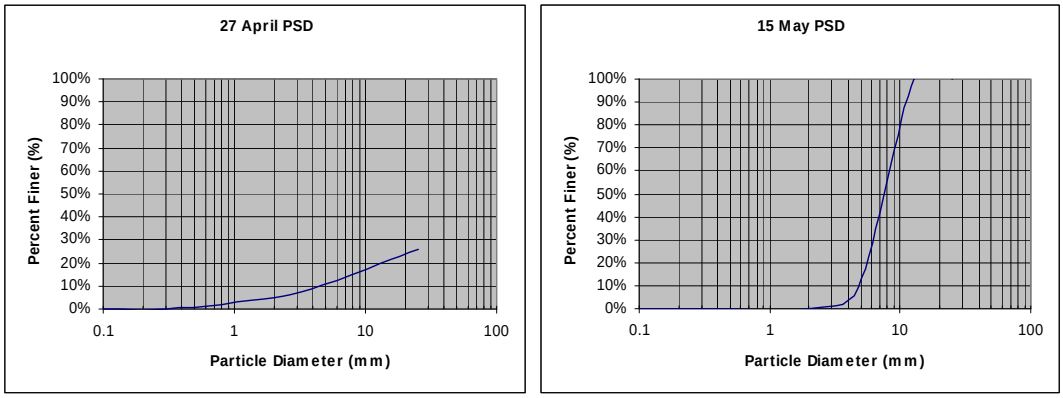

Figure A-4. Particle size distributions for bedload samples taken at Oak Leaf Ln. from 27 April through 15 May, 2006.

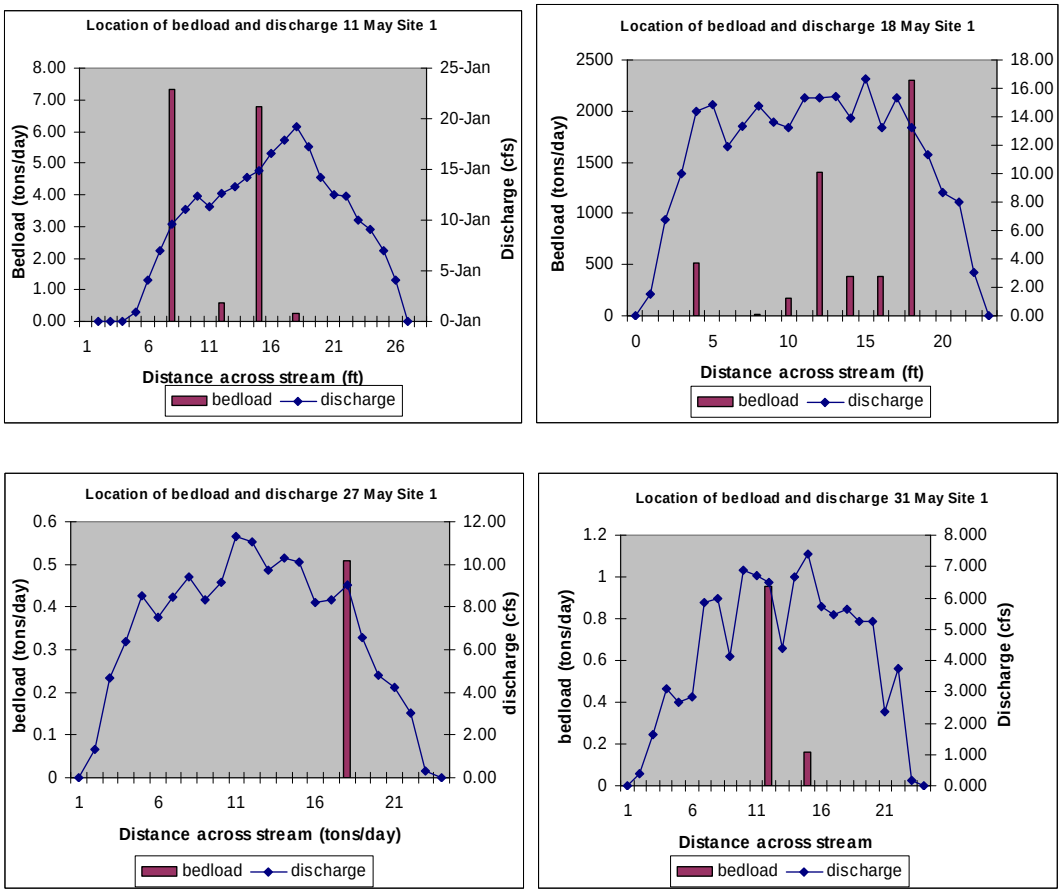

Figure A-5. Location of bedload movement and associated discharge for bedload samples taken at Site 1, 11 May through 31 May, 2006.

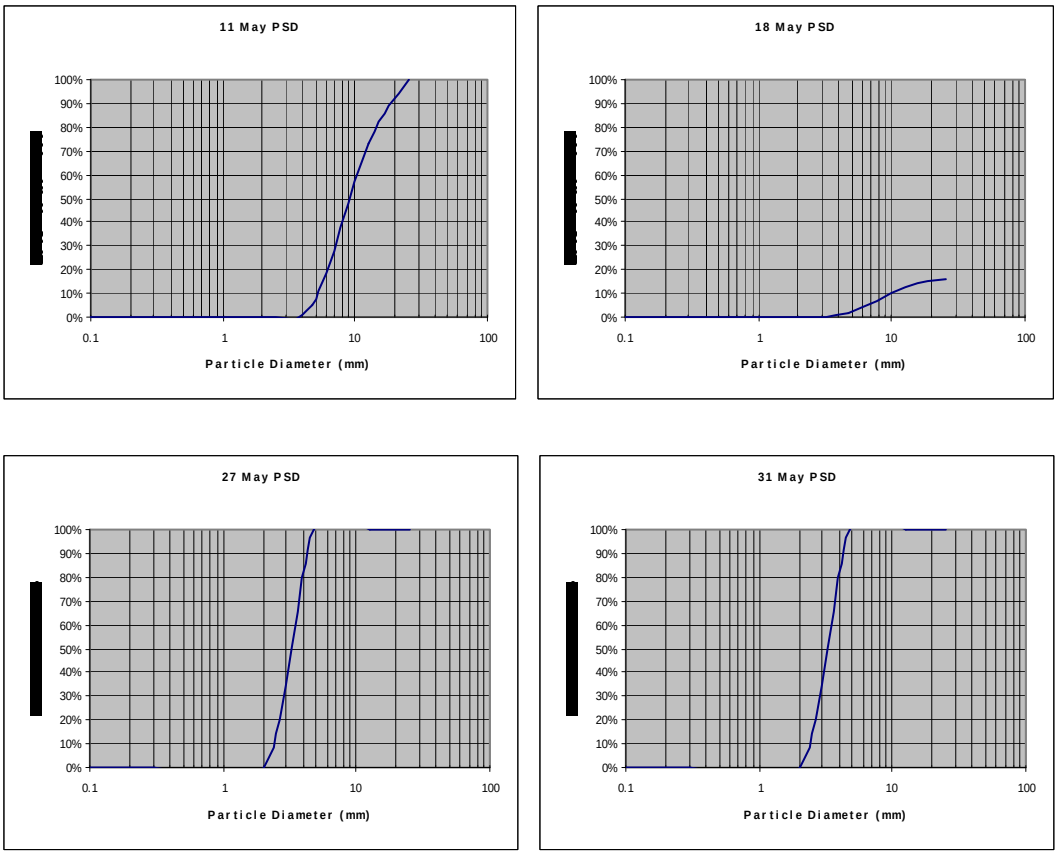

Figure A-6. Particle size distributions for bedload samples taken at Site 1, 11 May through 31 May, 2006.

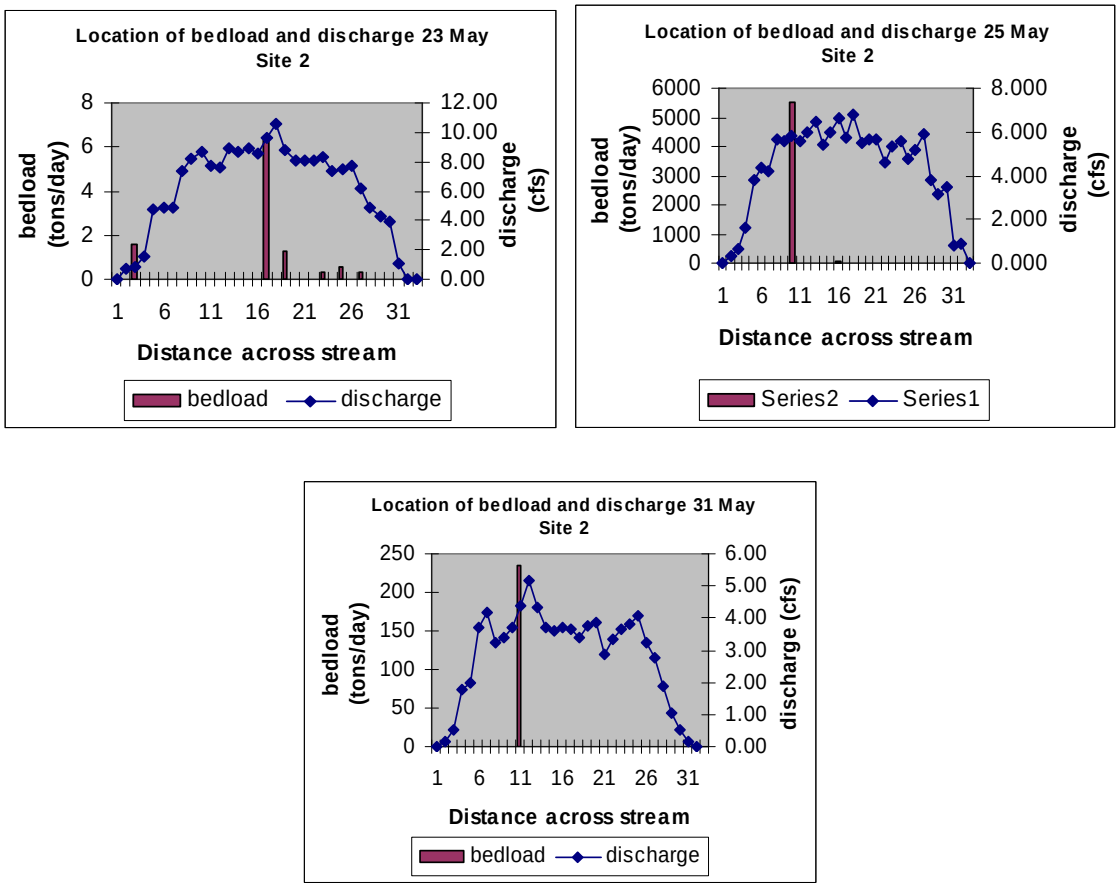

Figure A-7. Location of bedload movement and associated dischargees, for bedload samples taken at Site 2, 23 May through 31 May, 2006.

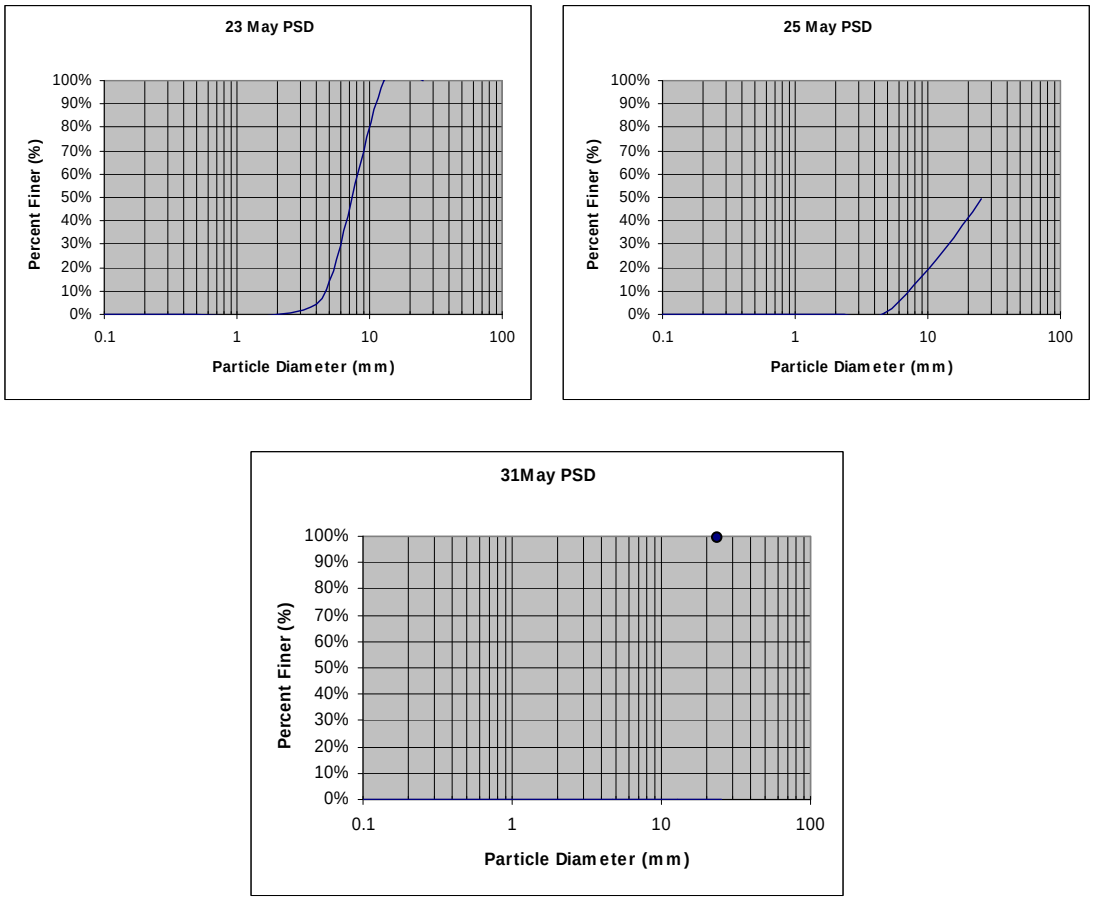

Figure A-8. Particle size distributions for bedload samples taken at Site 2, 23 through 31 May, 2006. The entire sample on 31 May consisted of one pebble, larger than the 24.5 mm sieve used.

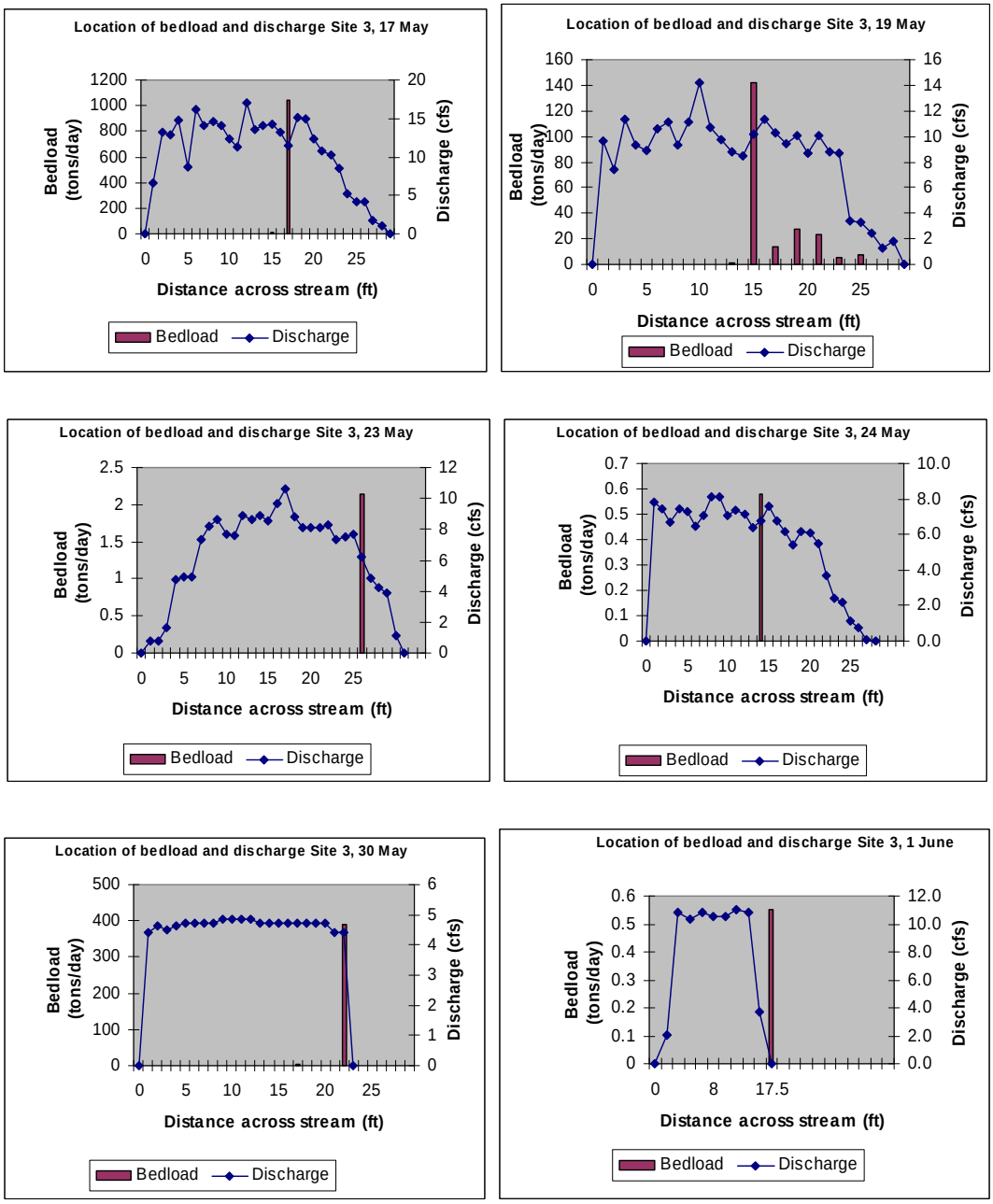

Figure A-9. Location of bedload and associated discharge for bedload samples taken at Site 3, 17 May through 1 June, 2006. The discharge on 30 May and 1 June was measure inside the large box culvert just upstream from the bedload sample site.

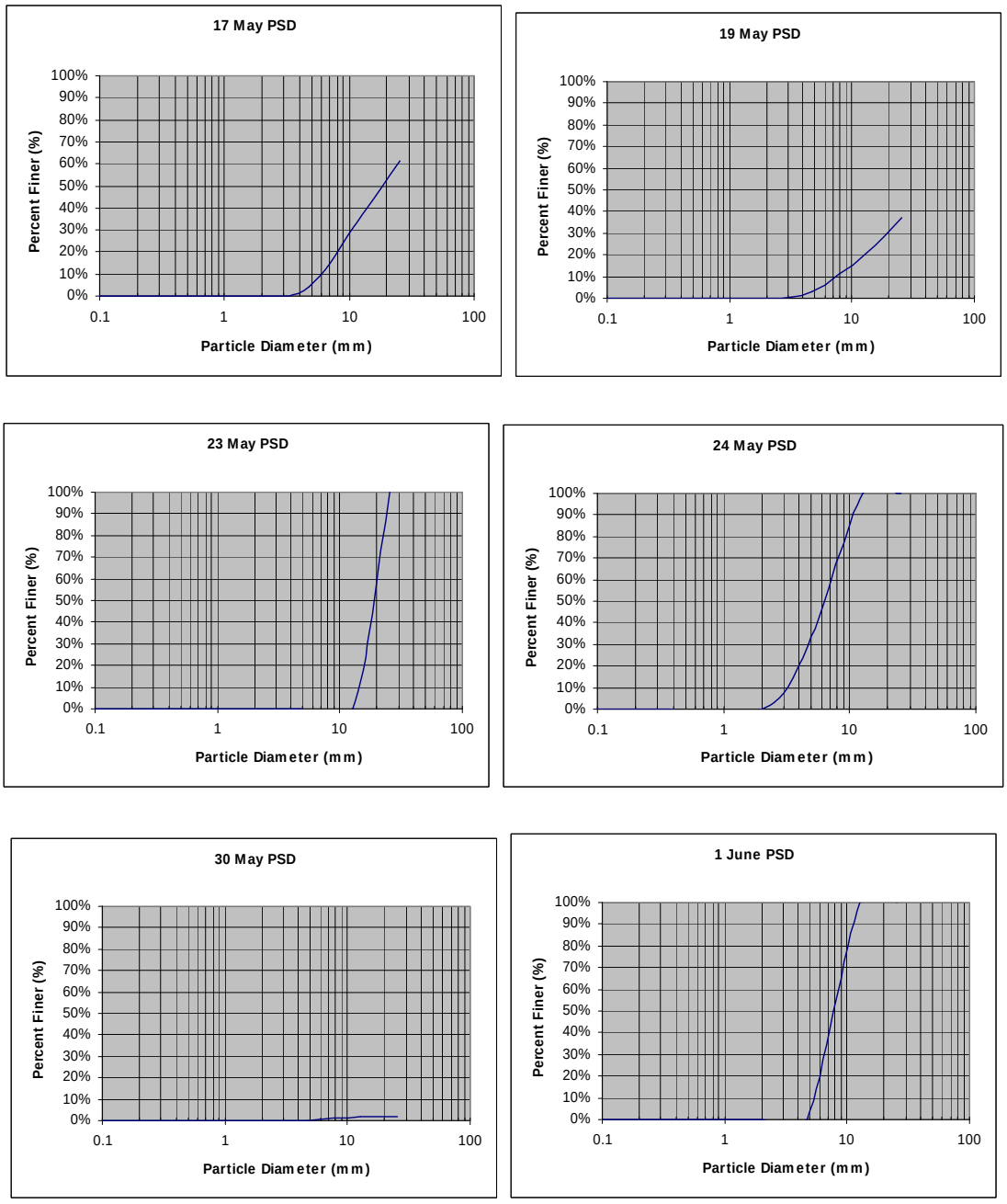

Figure A-10. Particle size distributions for bedload samples taken at Site 3, 17 May through 1 June, 2006.

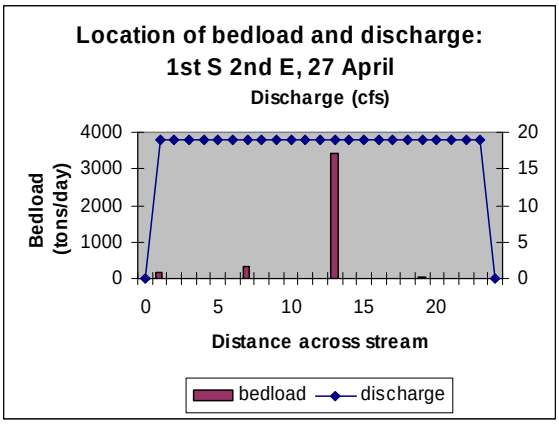

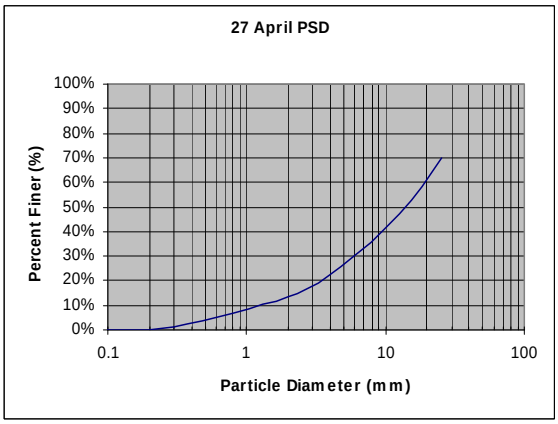

Figure A-11. Location of bedload movement, associated discharge, and particle size distribution of bedload sample taken at 1st S 2nd E bridge, 27 April 2006. The discharge was estimated using the "sunkist method", and assumed here to be uniformly distributed across the width of the stream.

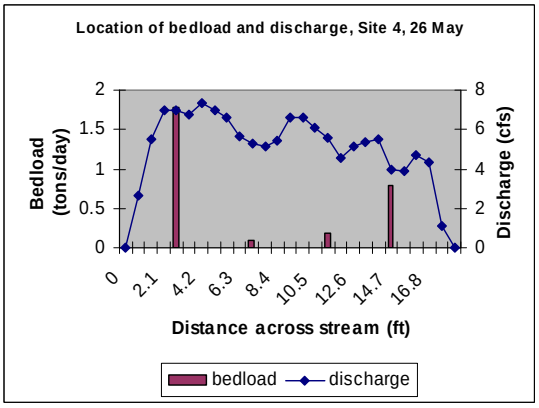

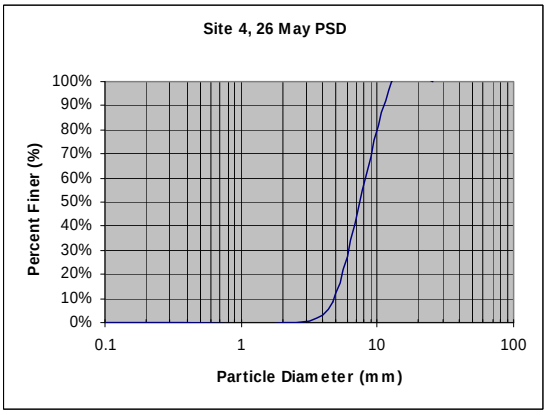

Figure A-12. Location of bedload, associated discharge, and particle size distribution of bedload sample taken at Site 4, 26 May 2006.

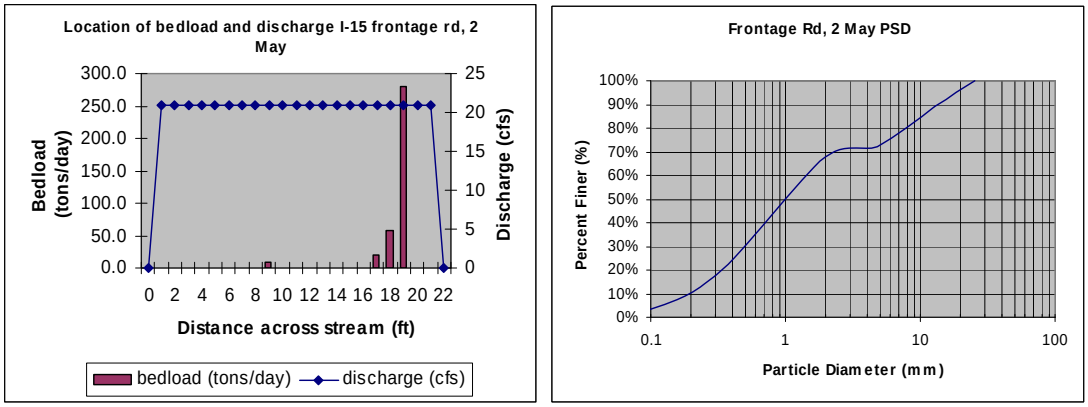

Figure A-13. Location of bedload movement, associated discharge, and particle size distribution of bedload sample taken at Frontage Rd, 27 April 2006. The current meter stopped working halfway across the stream, so the half we had done was doubled to estimate the total discharge, and was then assumed to be linearly distributed across the width of the stream.

Bridges

In order to facilitate bedload measurements, three portable bridges were built according to plans found in (Bunte et al 2007). Our bridges were each 32' long, and designed to span the creek a few feet at most above the water surface. Due to safety concerns with the unattended bridges being left out over the creek at night, all bridges were deployed each morning and retired to one side of the creek for storage at night. This was done out of safety concerns, as two of the three bridges were located near public access areas of the creek, and the other was located on private property where a family with young children lived. Bridges were deployed by with the following procedure:

- Two sturdy trees are located and a ½" diameter steel cable with two pulleys previously attached is strung between the two trees, using a come-along hand winch to provide tension (see Figure A-14 a).

- One end of the bridge (the end that will go to the opposite bank) is suspended from the main cable by two additional lengths of cable hooked to a pulley on the main cable (see Figure A-14 b).
- From this point, one person can lift the end that is not suspended and walk the bridge into position (see Figure A-14 c).
- Once the end of the bridge reaches the opposite bank, the cable is gradually loosened with the come-along and the bridge is lowered into position (see Figure A-14 d).

Figure A-14. A) Cable fastened around sturdy trees; B) hand winch used to tighten the cable; C) bridge is suspended by pulley, D) and pushed across the stream.

Appendix B Survey Work

We surveyed the length of Hobble Creek from the confluence of the right and left forks just upstream from Kelley's Grove (a public park) all the way to Utah Lake. Equipment used includes Top-Con© total stations, and handheld prism rods. Because a data collector was not available for our use, the data for each point was written by hand, and consisted of a vertical angle (from total station to prism), a horizontal angle (from previous to current prism points), and the distance from total station to prism. Points were taken at the start and end of each riffle, the deepest part of pools, and the start of glide sections. Figure B-1 and Figure B-2 illustrate our method for accomplishing this.

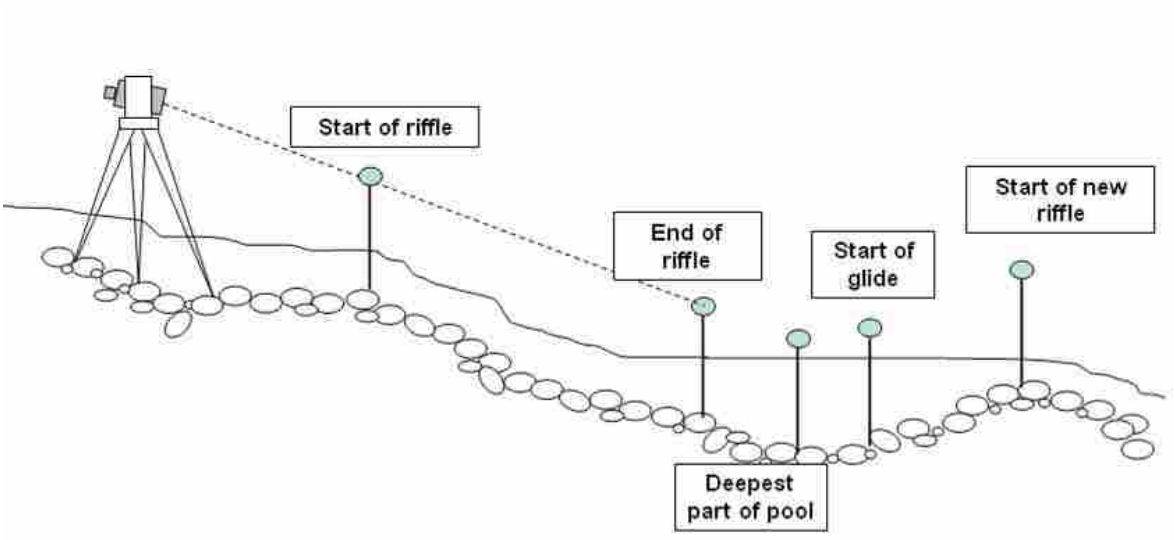

Figure B-1. Profile view of riffle-pool survey method.

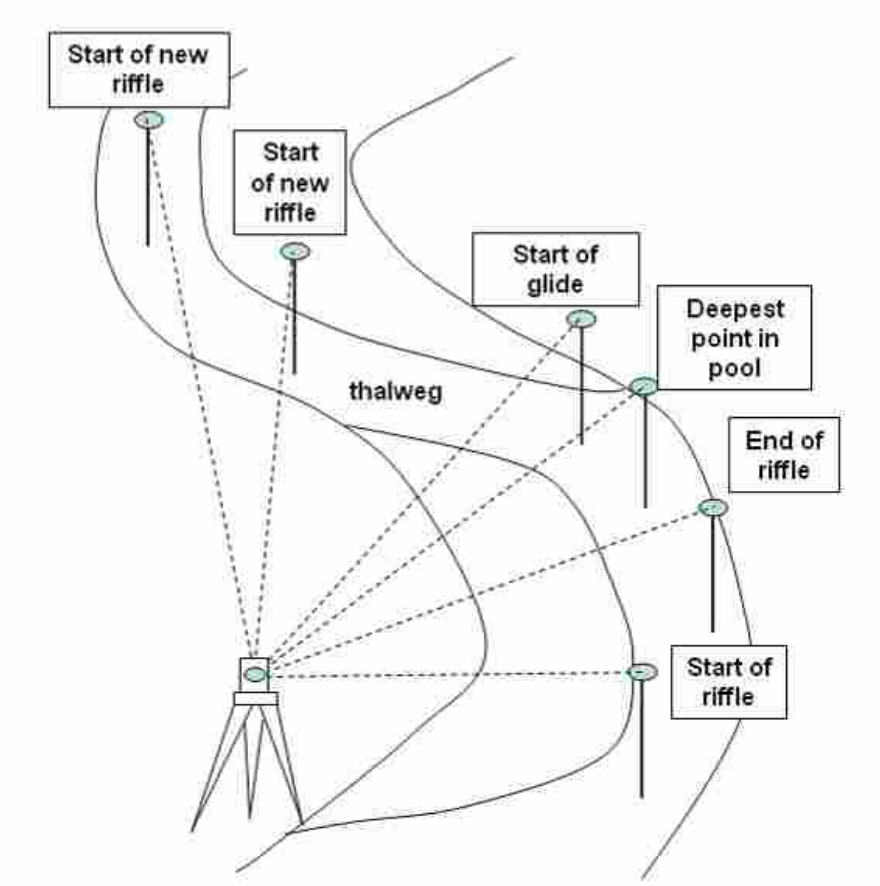

Figure B-2. Elevation view of riffle-pool survey method. Note that all points stay in the thalweg.

Using this method, every riffle, pool, and run was documented. At the point designated by a start of a riffle the water surface elevation was also taken. With water surface elevations from riffle to riffle we were able to determine the average water surface slope over a reach. Figure B-3 shows the profile of Hobble Creek from our survey data.

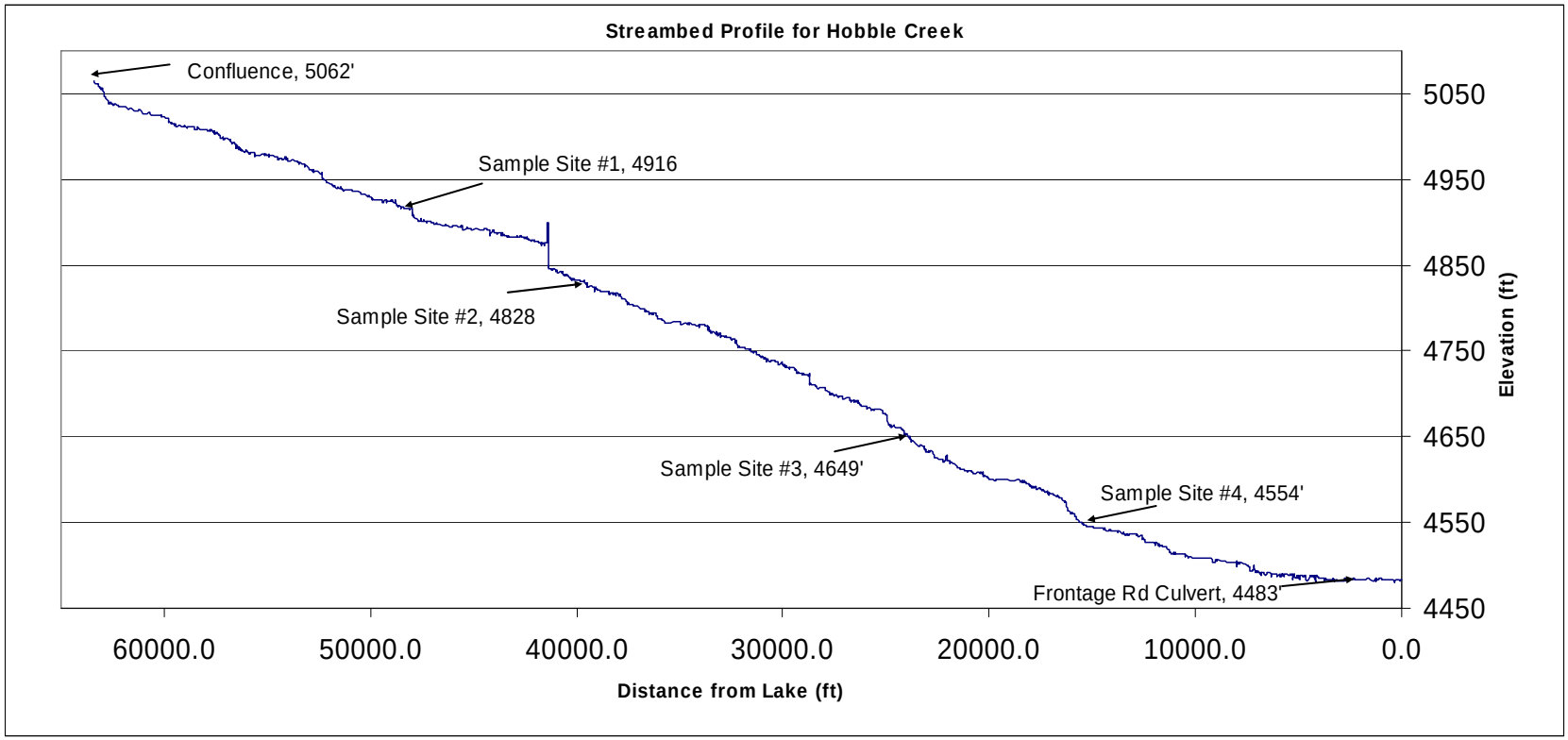

Figure B-3. Profile of Hobble Creek from confluence to Utah Lake.

Appendix C Pebble Counts

Since the predictive models that we used require the input of surface particle diameters, we performed pebble counts at each sample site. These were done according to pebble count guidelines as set forth in Bunte 2001 as well as guidelines written by Rosgen. The Rosgen method involves taking a reach of streambed 20-30 times the bankfull width long (we centered our pebble count reaches on our bedload sample site), and finding the approximate riffle-pool percentage. With this riffle-pool percentage known, we create 10 transects perpendicular to the stream, extending from the bankfull elevation on one side to bankfull elevation on the other side. The percentage of transects from riffles and pools corresponds to the riffle-pool percentage of that reach. So if the reach is 70% riffle and 30% pool, 7 of the 10 transects are taken in riffle areas and 3 area done in the pools. In each transect, 10 pebbles are counted, equally spaced between the two bankfull endpoints. Each pebble is selected without looking to limit bias. The following figures (Figure C-1 through C-8) show bed surface material particle size distributions developed for each sample site.

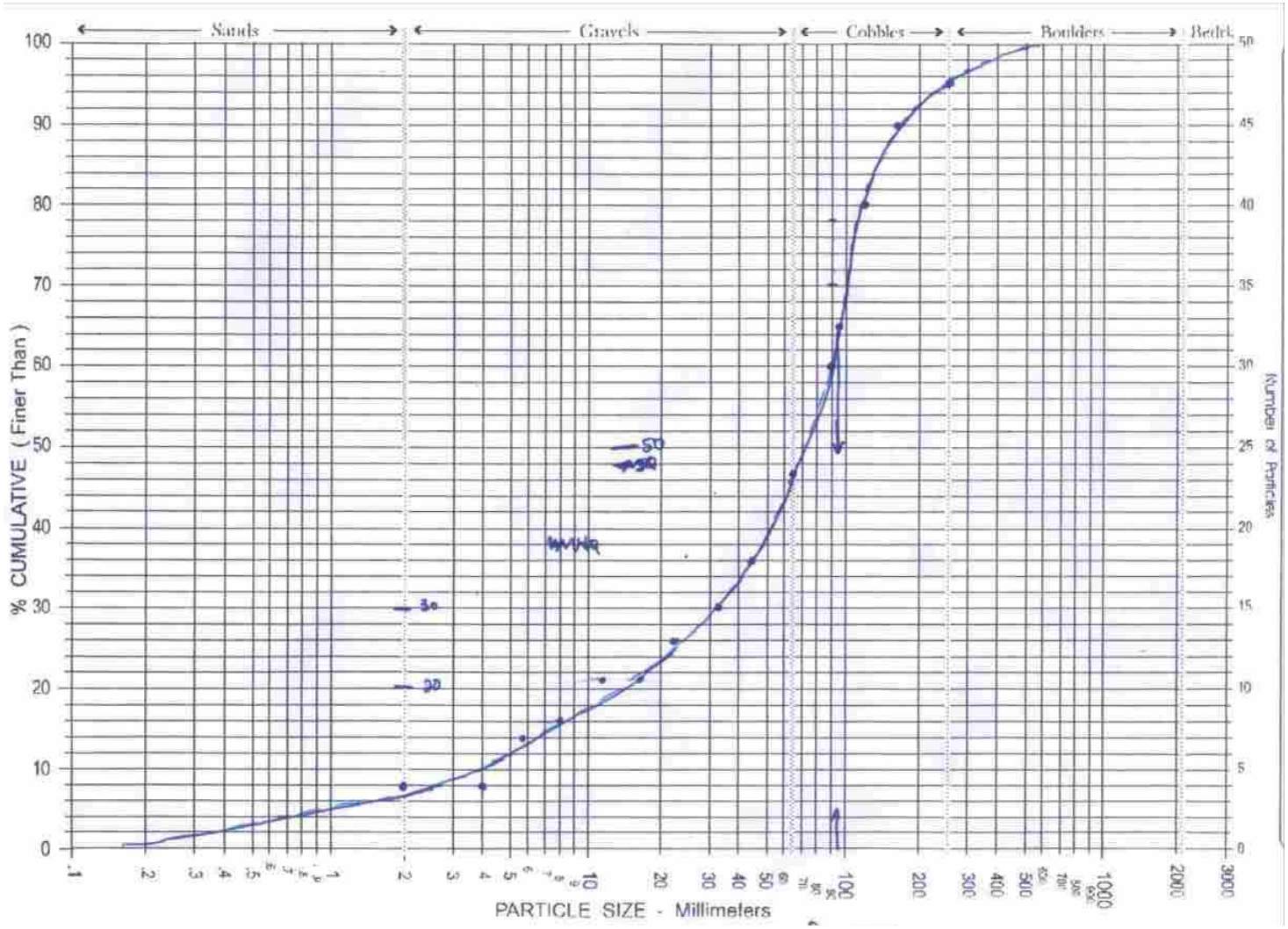

Figure C-1. Particle size distribution chart for the reach encompassing the bedl;oad sample site at Golf Course Bridge.

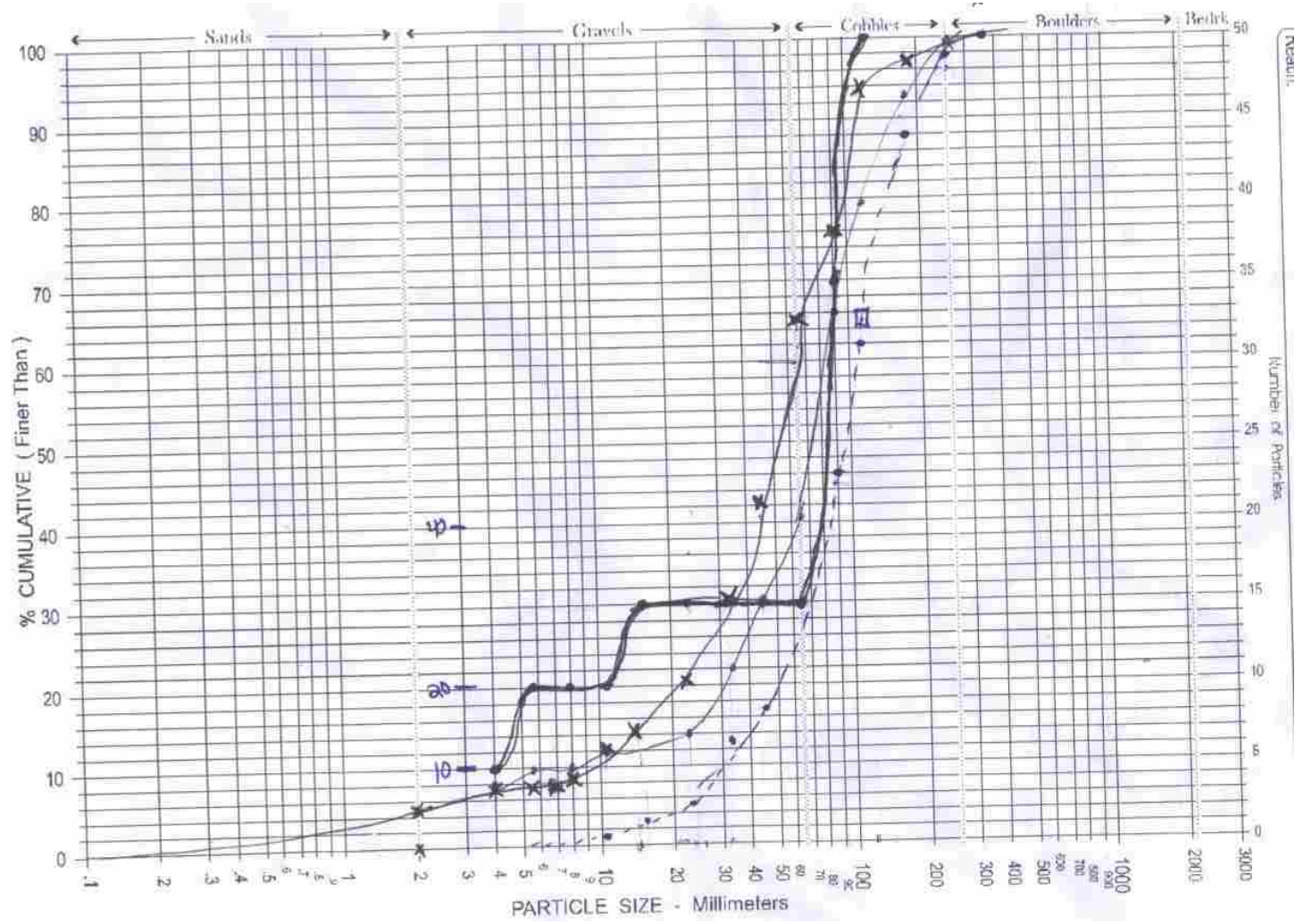

Figure C-2. Particle size distribution for reach encompassing bedload sample Site 1.

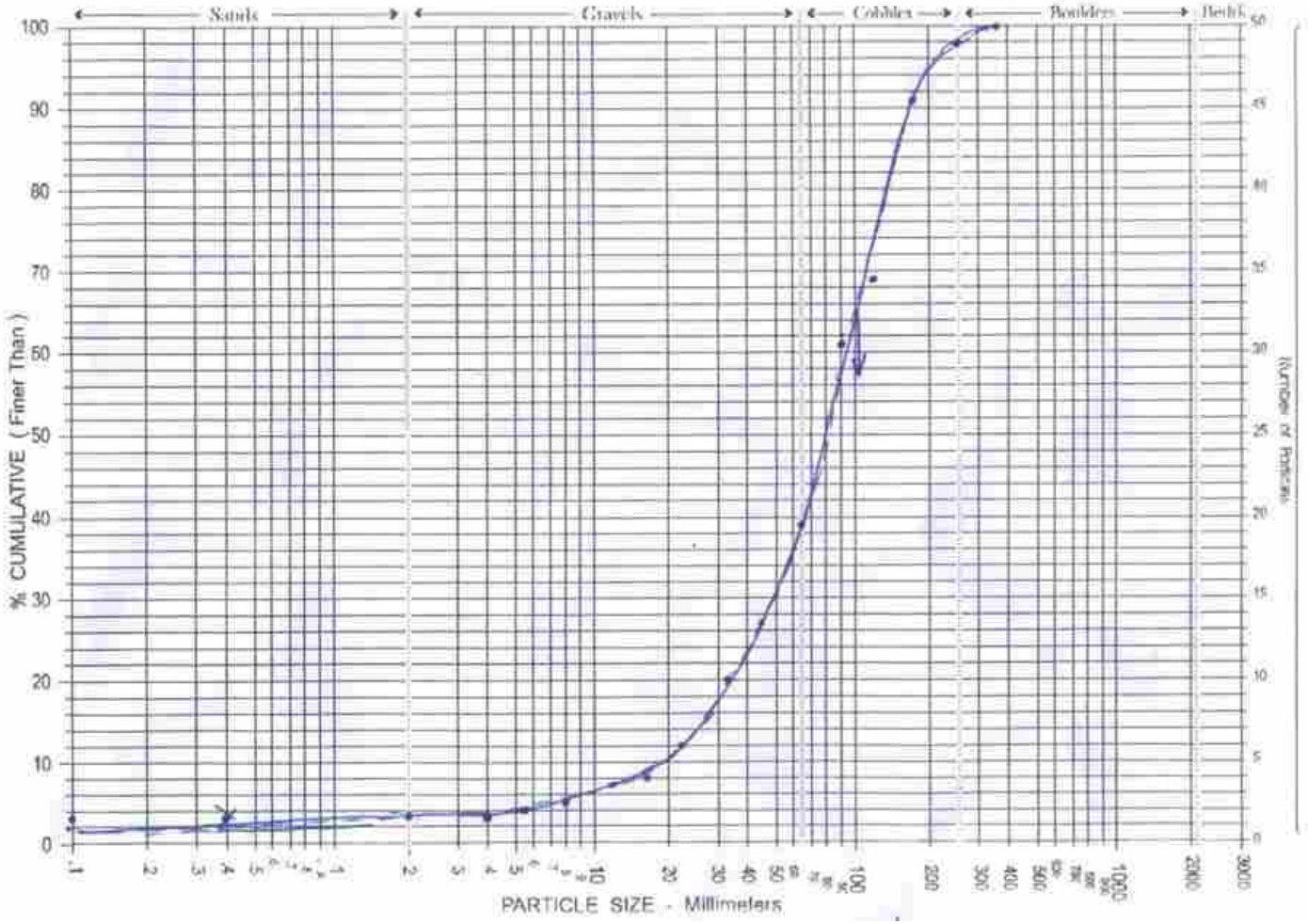

Figure C-3. Particle size distribution for the reach encompassing the Oak Leaf Lane sample site.

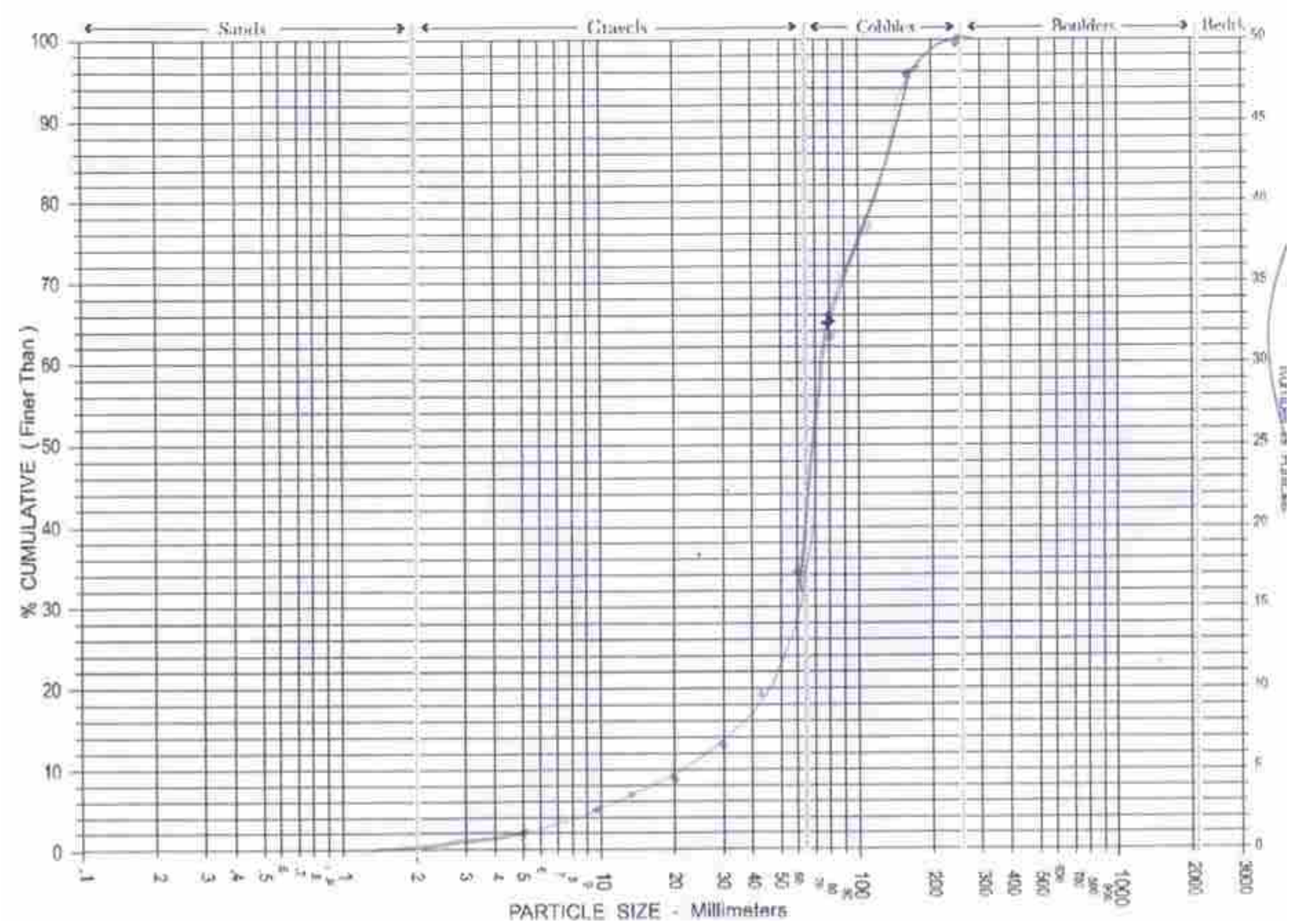

Figure C-4. Particle size distribution for the reach encompassing sample Site 2.

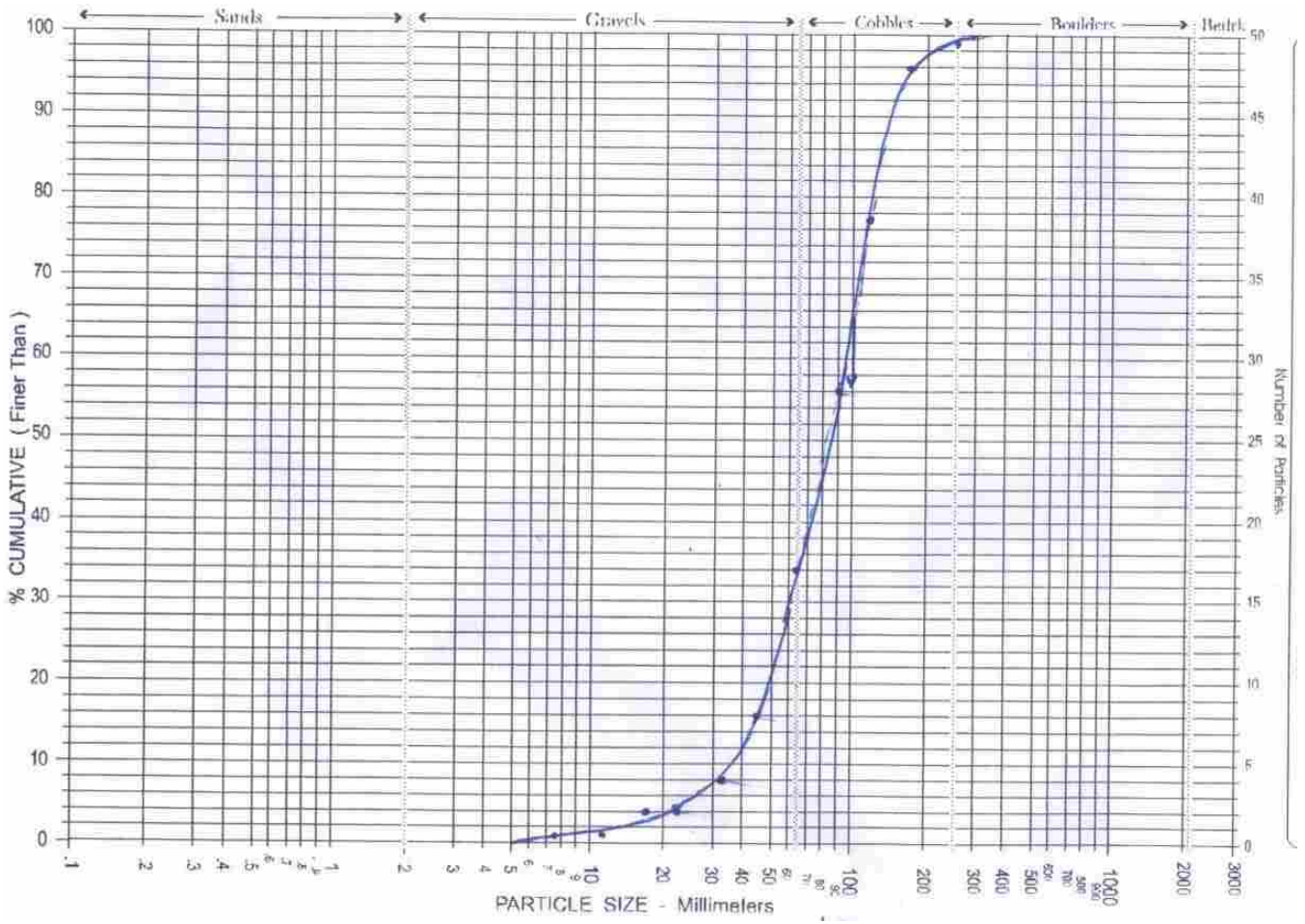

Figure C-5. Particle size distribution chart for the reach encompassing the bedload sample site located at 1st S 2nd E.

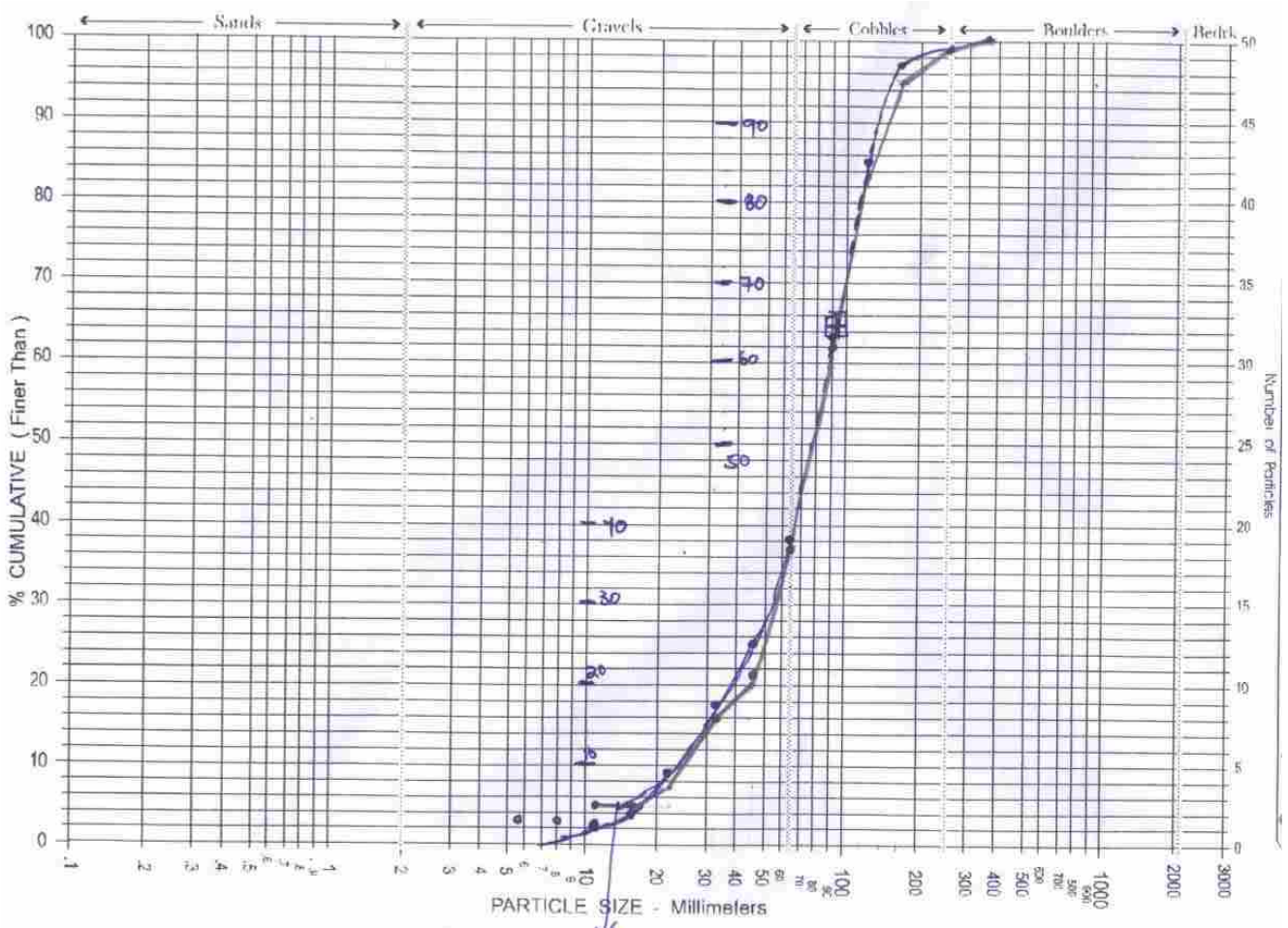

Figure C-6. Particle size distribution for bedload sample site 4.

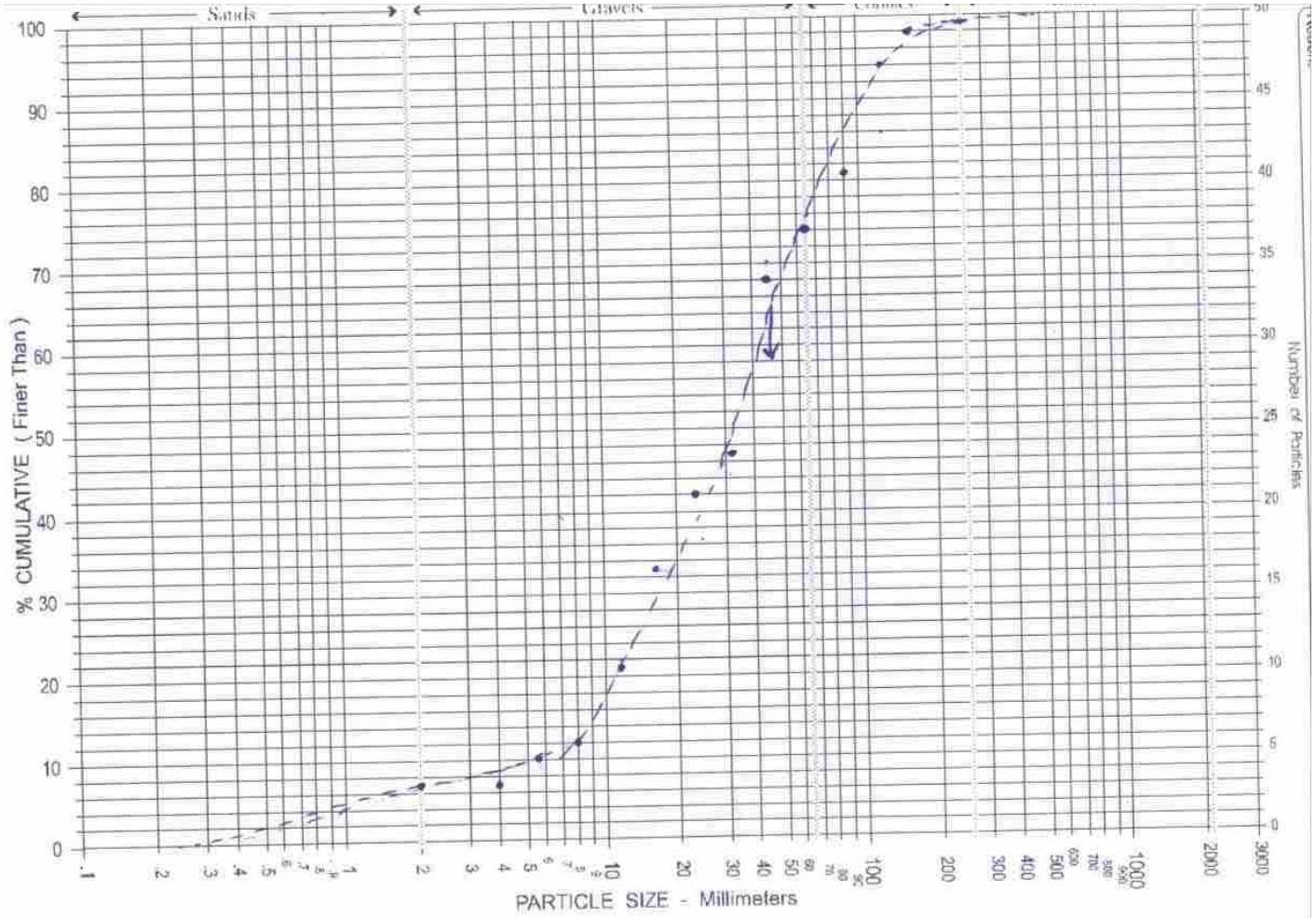

Figure C-7. Particle size distribution for reach immediately upstream of the I-15 culvert.

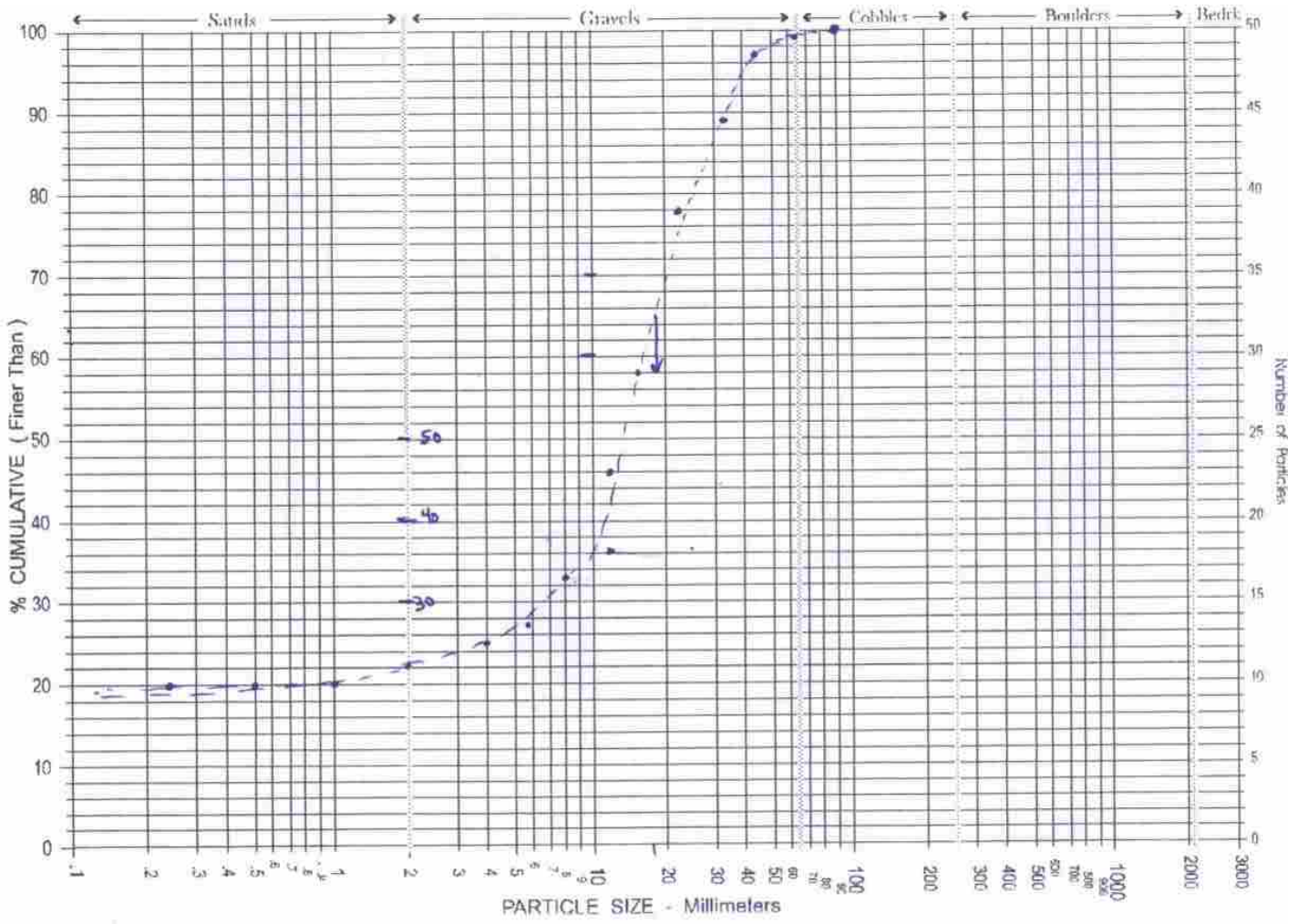

Figure C-8. Particle size distribution for the reach immediately below the I-15 culvert.

These preceding figures can be summarized in the following figure that illustrates their distributions relative to each other:

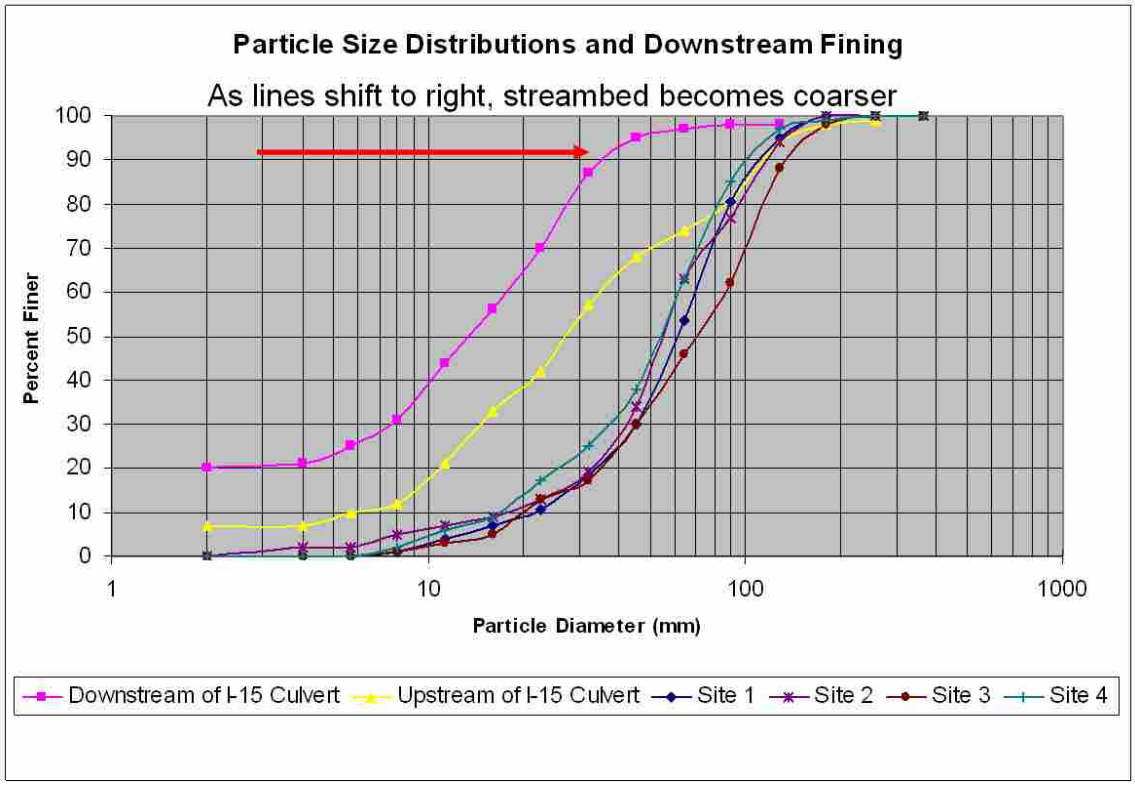

Figure C-9. Comparison of bed surface particle size distributions from 6 locations of Hobble Creek.

Appendix D Subsurface Samples

The Bathurst equation requires the D_{50} of the subsurface as one of the input parameters. Subsurface samples were taken at Sites 1-3, and particle size distributions were obtained from each.

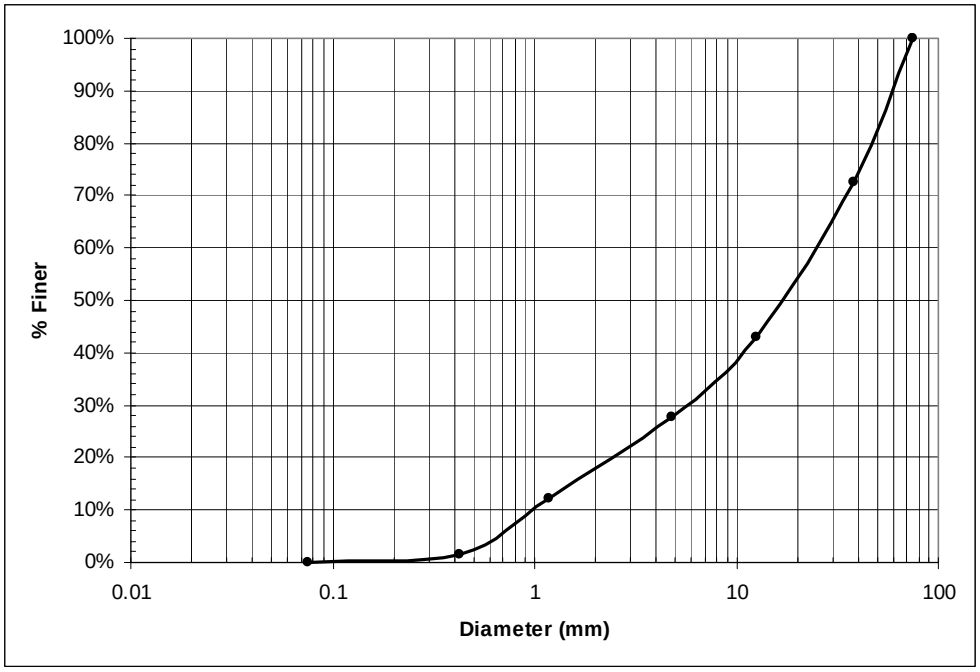

Figure D-1. Particle size distribution for Site 1 subsurface.

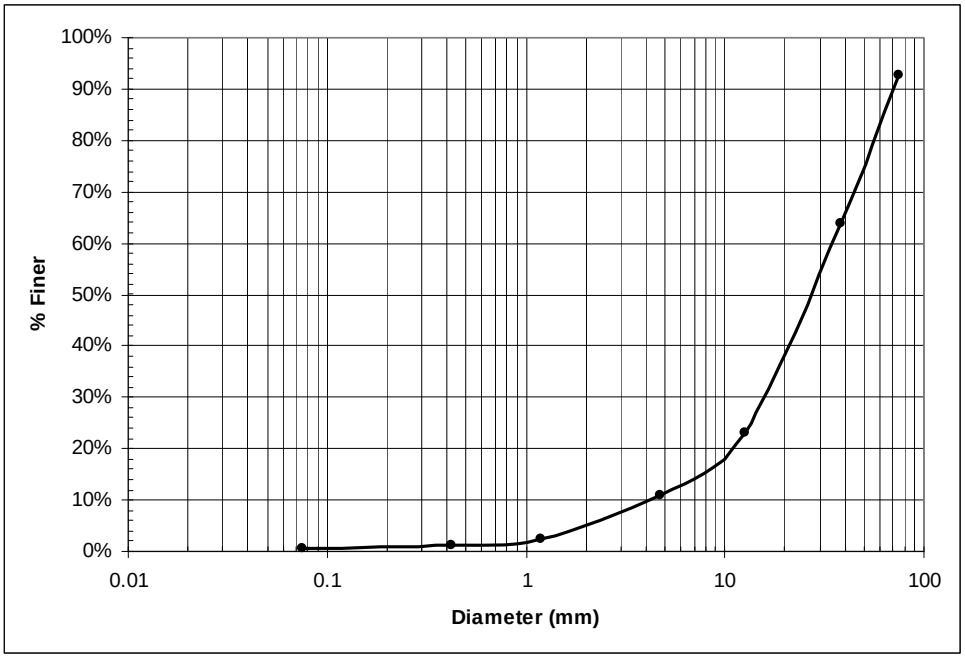

Figure D-2. Particle size distribution for Site 2 subsurface.

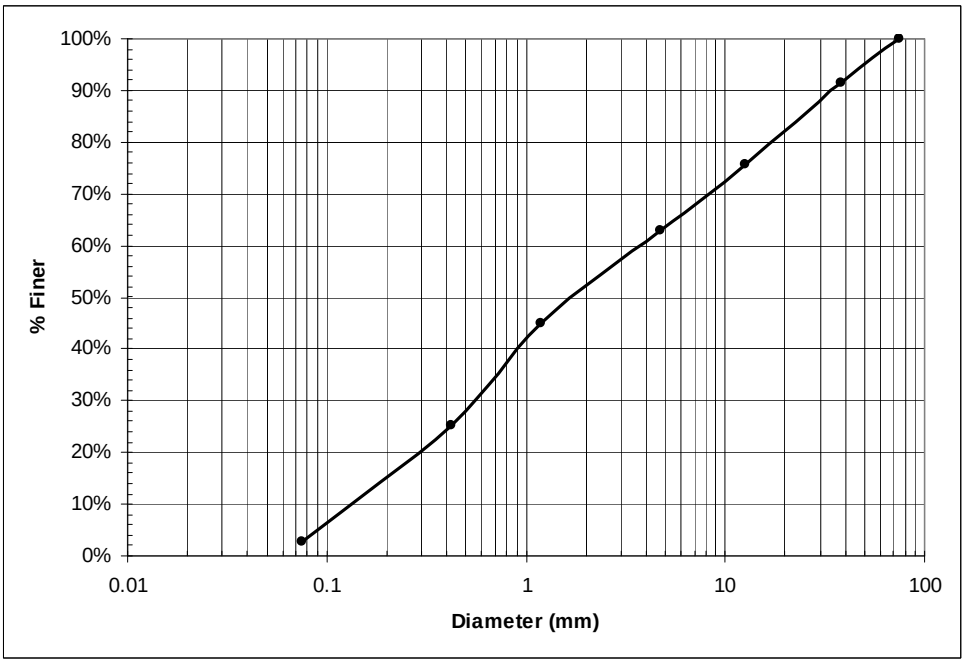

Figure D-3. Particle size distribution for Site 3 subsurface.

Figure D-4. Photo of Site 1 subsurface sample area.

Figure D-5. Photo of Site 2 subsurface sample area.

Figure D-6. Photo of Site 3 subsurface sample area.

Appendix E Biological Data

The following tables (E-1 through E-4) present the geographic coordinates (in deg-min-sec) of the sample sites where food resource characterization and minnow density were sampled.

Table E-1. Coordinates for sampling sites in Open zone.

Zone: Open Lake		
Transect	**Sample Site**	**Coordinates**
40°11'18.0"	50	111 40 43.1
	100	111 40 40.8
	150	111 40 38.4
40°11'12.0"	50	111 40 54.2
	100	111 40 56.1
	150	111 40 58.4
40°11'6.0"	50	111 41 2.1
	100	111 41 3.9
	150	111 41 6.2

Table E-2. Coordinates for sampling sites in Sparse zone.

Zone: Sparse Vegetation		
Transect	**Sample Site (E to W)**	**Coordinates**
40°11'18.0"	¼	111 40 21.6
	½	111 40 7.0
	¾	111 39 52.4
40°11'12.0"	¼	111 39 49.4
	½	111 40 10.3
	¾	111 40 31.2
40°11'6.0"	¼	111 40 23
	½	111 40 37.5
	¾	111 40 48.3

Table E-3. Coordinates for sampling sites in Dense zone.

Zone: Dense Vegetation		
Transect	**Sample Site**	**Coordinates**
40°11'18.0"	50	111 39 35.6
	100	111 39 33.7
	150	111 39 31.5
40°11'12.0"	50	111 39 26.5
	100	111 39 24.2
	150	111 39 22.2
40°11'6.0"	50	111 40 8.1
	100	111 40 6.0
	150	111 40 3.9

Table E-4. Coordinates for sampling sites in Creek zone.

Zone: Creek			
Transect	**Sample Site**	**Coordinates**	
		Latitude	**Longitude**
#6	A	111°39'0.1"	40°11'6.6"
	B	111°39'0.1"	40°11'6.6"
	C	111°39'0.1"	40°11'6.6"
#27	D	111°39'4.0"	40°11'16.9"
	E	111°39'4.0"	40°11'16.9"
	F	111°39'4.0"	40°11'16.9"
#18	G	111°39'18.9"	40°11'23.4"
	H	111°39'18.9"	40°11'23.4"
	I	111°39'18.9"	40°11'23.4"

Plankton

Zooplankton sample data from June and August are shown below in Tables E-5 and E-6. The data in columns 4 through 13 contain the total number of each species found at each sample site. As described above, samples were taken and subdivided to facilitate counting the organisms in the total sample. Each column below contains the total number of each species found in the sample. Eleven organisms were identified to the genus level in zooplankton samples.

Benthos

Benthic invertebrates sample data are shown in Tables E-7 and E-8. The data in columns 5 through 17 contain the total number of each species found at each sample site.

As described above, samples were taken and subdivided to facilitate enumeration procedures. 12 taxonomic groups were identified to the genus level in benthos samples.

Fish Density Data

Existing fish density was determined through minnow traps deployed at six sample sites in each zone. These sites were randomly selected from the nine sites where plankton sampling occurred, and traps were left for 24 hours. Table E-9 presents this data in tabular form.

Table E-5. June zooplankton sample data.

Date	Transect	Zone name	Sites / Replicate	Oligochaetes	Chironomids	Ostracods	Corixids	Harpactacoids	Hematodes	Rotifers	Copepods	Nauplii	Cladocerans	Total
27-Jun-06	6	open	150	0	0	0	2	0	0	1036	451	90	254	1833
26-Jun-06	6	open	100	0	0	0	0	0	0	951	258	210	274	1693
27-Jun-06	6	open	50	0	0	0	0	0	0	354	119	98	93	664
26-Jun-06	6	sparse	1/4	0	0	0	0	5	1	400	734	1	290	1431
26-Jun-06	6	sparse	1/2	1	1	14	3	0	0	27	440	187	212	895
28-Jun-06	6	sparse	3/4	0	0	0	0	0	0	611	94	0	376	1081
27-Jun-06	6	dense	50	0	0	0	0	0	0	461	56	0	282	799
27-Jun-06	6	dense	100	0	0	0	0	0	0	1297	85	0	160	1541
27-Jun-06	6	dense	150	0	19	0	0	0	9	273	38	0	244	583
28-Jun-06	12	open	150	0	0	3	0	0	0	189	285	179	502	1158
28-Jun-06	12	open	100	0	0	0	0	0	0	922	377	496	554	2349
28-Jun-06	12	open	50	0	0	4	0	0	0	354	352	379	572	1661
28-Jun-06	12	sparse	1/4	0	0	2	0	0	0	151	386	464	533	1537
28-Jun-06	12	sparse	1/2	0	0	0	0	0	0	347	272	56	404	1080
28-Jun-06	12	sparse	3/4	0	19	28	0	0	0	704	75	516	2131	3474
27-Jun-06	12	dense	50	0	0	9	9	0	0	0	0	0	141	160
27-Jun-06	12	dense	100	0	17	9	0	0	0	43	34	17	60	179
29-Jun-06	12	dense	150	0	0	19	9	0	0	160	742	460	648	2038
28-Jun-06	18	open	150	0	0	3	0	0	0	39	249	129	183	603
28-Jun-06	18	open	100	0	0	8	0	0	0	22	192	102	137	461
28-Jun-06	18	open	50	0	0	0	0	4	0	166	241	269	167	848
29-Jun-06	18	sparse	1/4	0	0	3	0	6	0	9	203	313	108	641
29-Jun-06	18	sparse	1/2	0	0	0	0	1	0	1	3	30	37	73
27-Jun-06	18	sparse	3/4	0	1	1	0	0	0	1	5	5	29	41
28-Jun-06	18	dense	50	0	0	0	0	0		66	47	47	535	695
28-Jun-06	18	dense	100	9	9	0	0	0	0	282	75	19	347	742
28-Jun-06	18	dense	150	0	0	0	0	0	0	0	0	0	0	0
3-Jul-06	#6	creek	a	0	0	0	0	0	0	0	0	0	0	0
3-Jul-06	#6	creek	b	0	0	0	0	0	0	0	0	0	0	0
3-Jul-06	#6	creek	c	0	0	0	0	0	0	0	0	0	0	0
3-Jul-06	#27	creek	d	0	0	0	0	0	0	0	0	9	0	9
3-Jul-06	#27	creek	e	9	0	0	0	0	47	169	9	0	9	244
3-Jul-06	#27	creek	f	0	0	0	0	0	0	0	0	0	0	0
3-Jul-06	#18	creek	g	0	0	0	0	0	0	122	9	17	17	165
3-Jul-06	#18	creek	h	0	0	0	0	0	47	281	42	0	28	398
3-Jul-06	#18	creek	i	0	0	0	0	0	0	208	16	0	32	256

Table E-6. August zooplankton data.

Date	Transect	Zone name	Sites/Replicate	Oligochaetes	Chironomids	Ostracods	Corixids	Harpacticoids	Nematodes	Rotifers	Copepods	Nauplii	Cladocerans	Total
8-Aug-06	6	open	150	0	0	0	0	0	0	10252	1305	913	85	12554
8-Aug-06	6	open	100	missing	missing	missing	missing	missing	missing	missing	missing	missing	missing	0
8-Aug-06	6	open	50	0	0	3	0	0	0	5167	932	621	79	6802
8-Aug-06	6	sparse	1/4	0	0	0	0	0	0	119	796	0	0	915
8-Aug-06	6	sparse	1/2	0	0	0	0	0	0	64	371	204	124	763
8-Aug-06	6	sparse	3/4	0	2	2	0	0	0	112	21	66	78	280
8-Aug-06	6	dense	50	0	0	0	0	0	0	38	9	9	113	169
8-Aug-06	6	dense	100	9	0	0	0	0	0	160	56	19	38	282
8-Aug-06	6	dense	150	0	0	28	0	0	0	216	9	19	122	394
8-Aug-06	12	open	150	0	0	0	0	0	0	134	286	287	33	741
8-Aug-06	12	open	100	0	0	0	0	0	0	1678	319	309	50	2356
8-Aug-06	12	open	50	0	0	0	0	0	0	213	312	385	31	940
8-Aug-06	12	sparse	1/4	0	0	0	0	0	0	232	285	490	71	1078
8-Aug-06	12	sparse	1/2	0	0	0	0	0	0	38	460	150	28	676
8-Aug-06	12	sparse	3/4	0	0	1	0	0	0	1	225	153	5	387
8-Aug-06	12	dense	50	0	0	0	0	0	0	169	94	85	0	347
8-Aug-06	12	dense	100	9	0	0	0	0	0	47	263	47	0	366
8-Aug-06	12	dense	150	0	0	0	0	0	0	0	0	0	0	0
9-Aug-06	18	open	150	0	0	0	0	0	0	719	277	328	55	1378
8-Aug-06	18	open	100	0	0	2	0	0	0	671	261	327	91	1352
8-Aug-06	18	open	50	0	0	0	0	0	0	605	315	480	113	1513
8-Aug-06	18	sparse	1/4	0	0	0	0	0	0	138	242	557	28	965
8-Aug-06	18	sparse	1/2	0	0	19	0	0	0	0	197	948	9	1174
8-Aug-06	18	sparse	3/4	0	0	0	0	0	1	8	134	546	3	692
9-Aug-06	18	dense	50	0	0	0	0	0	0	19	9	9	0	38
8-Aug-06	18	dense	100	9	0	0	0	0	0	0	56	19	0	85
9-Aug-06	18	dense	150	0	0	0	0	0	0	122	85	66	9	282
9-Aug-06	#6	creek	a	missing	missing	missing	missing	missing	missing	missing	missing	missing	missing	0
9-Aug-06	#6	creek	b	0	0	0	9	0	0	0	0	0	0	9
9-Aug-06	#6	creek	c	0	0	0	0	0	0	0	9	0	9	19
9-Aug-06	#27	creek	d	0	0	0	0	0	0	0	9	0	9	19
9-Aug-06	#27	creek	e	0	9	0	0	0	0	9	19	9	0	47
9-Aug-06	#27	creek	f	0	0	0	0	0	0	0	9	19	0	28
9-Aug-06	#18	creek	g	0	0	0	0	0	0	0	0	0	0	0
9-Aug-06	#18	creek	h	0	0	0	0	0	0	0	0	0	0	0
9-Aug-06	#18	creek	i	0	0	0	0	0	0	0	0	0	19	19

Table E-7. June benthos data

Date	Transect	Zone name	Sites/Replicate	Oligochaetes	Chironomids	Ostracods	Cosinids	Harpacticoids	Microcaddis	Turbellaria	Amphipods	Nematodes	Rotifers	Copepods	Nauplii	Cladocerans	Total
27-Jun-06	6	open	150	0	0	8	0	0	0	0	0	40	0	0	0	14	62
26-Jun-06	6	open	100	2	0	6	0	0	0	0	0	25	0	0	0	1	33
27-Jun-06	6	open	50	1	1	7	0	1	0	0	0	22	0	1	0	0	33
26-Jun-06	6	sparse	1/4	0	0	2	0	0	0	0	0	10	0	1	0	0	13
26-Jun-06	6	sparse	1/2	47	3	2	0	12	0	0	0	4	0	7	0	0	75
28-Jun-06	6	sparse	3/4	0	18	8	2	5	1	3	5	109	0	0	0	1	151
27-Jun-06	6	dense	50	25	4	13	0	1	0	0	0	0	0	0	0	0	43
27-Jun-06	6	dense	100	3	0	7	0	2	0	0	0	0	0	0	0	0	12
27-Jun-06	6	dense	150	0	0	12	0	0	0	0	0	0	0	0	0	0	12
28-Jun-06	12	open	150	5	1	0	0	0	0	0	0	25	0	0	0	0	31
28-Jun-06	12	open	100	18	8	3	0	0	0	0	0	26	0	0	0	0	55
28-Jun-06	12	open	50	5	0	0	0	0	0	0	0	12	0	10	0	0	27
28-Jun-06	12	sparse	1/4	9	40	32	5	38	1	7	23	9	0	0	0	0	165
28-Jun-06	12	sparse	1/2	9	18	16	8	10	6	12	11	13	0	1	0	0	104
28-Jun-06	12	sparse	3/4	19	86	16	0	7	1	9	30	33	0	0	0	0	201
27-Jun-06	12	dense	50	2	1	17	0	0	0	0	0	16	0	0	0	0	35
27-Jun-06	12	dense	100	2	2	21	0	0	0	0	0	1	0	3	0	0	29
29-Jun-06	12	dense	150	6	1	17	0	1	0	0	0	1	0	2	0	1	28
28-Jun-06	18	open	150	1	14	3	0	0	0	0	0	1	0	0	0	0	19
28-Jun-06	18	open	100	2	16	0	0	2	0	0	0	3	0	0	0	0	22
28-Jun-06	18	open	50	2	12	0	0	0	0	0	0	11	0	0	0	0	25
29-Jun-06	18	sparse	1/4	23	0	6	0	0	0	0	0	7	0	0	0	0	36
29-Jun-06	18	sparse	1/2	13	0	18	0	1	0	0	0	2	0	0	0	0	33
27-Jun-06	18	sparse	3/4	5	0	30	0	0	0	0	0	8	0	0	0	0	43
28-Jun-06	18	dense	50	17	0	40	0	1	0	0	0	0	0	0	0	0	58
28-Jun-06	18	dense	100	13	1	9	0	0	0	0	0	5	0	0	0	0	28
28-Jun-06	18	dense	150	9	3	7	0	0	0	0	0	5	0	0	0	0	23
3-Jul-06	#6	creek	a	7	43	1	0	3	0	0	3	120	0	0	0	0	177
3-Jul-06	#6	creek	b	44	26	0	0	6	0	0	0	51	0	0	0	0	127
3-Jul-06	#6	creek	c	12	47	0	0	8	0	1	4	41	0	0	0	0	113
3-Jul-06	#27	creek	d	53	5	0	0	60	0	0	0	33	0	0	0	0	152
3-Jul-06	#27	creek	e	100	8	6	0	51	0	0	0	35	0	0	0	0	200
3-Jul-06	#27	creek	f	77	7	2	0	39	0	0	0	19	0	0	0	0	143
3-Jul-06	#18	creek	g	9	3	0	0	10	1	0	0	5	0	0	0	0	28
3-Jul-06	#18	creek	h	49	2	0	0	20	0	0	0	15	0	2	0	0	87
3-Jul-06	#18	creek	i	3	0	0	0	62	0	0	0	86	0	0	0	0	151

Table E-8. August benthos data.

Date	Transect	Zone name	Sites/Replicate	Oligochaetes	Chironomids	Ostracods	Corixids	Harpacticoids	Microcaddis	Turbellaria	Amphipods	Nematodes	Rotifers	Copepods	Nauplii	Cladocerans	Total
8-Aug-06	6	open	150	1	0	0	0	0	0	0	0	0	0	1	0	0	3
8-Aug-06	6	open	100	2	1	2	0	0	0	0	0	45	0	0	0	0	49
8-Aug-06	6	open	50	missing	missing	missing	missing	missing	missing	missing	missing	missing	missing	missing	missing	missing	0
8-Aug-06	6	sparse	1/4	1	0	4	0	0	0	0	0	3	0	0	0	0	8
8-Aug-06	6	sparse	1/2	1	0	0	0	0	0	0	0	3	0	0	0	0	4
8-Aug-06	6	sparse	3/4	1	3	0	0	0	0	0	0	5	0	0	0	0	8
8-Aug-06	6	dense	50	1	0	5	0	0	0	0	0	3	0	0	0	0	10
8-Aug-06	6	dense	100	3	0	27	0	0	0	0	0	0	0	0	0	0	30
8-Aug-06	6	dense	150	4	0	24	0	0	0	0	0	5	0	0	0	0	33
8-Aug-06	12	open	150	1	0	10	0	0	0	0	0	38	0	0	0	0	49
8-Aug-06	12	open	100	10	6	10	0	0	0	0	0	67	0	0	0	0	93
8-Aug-06	12	open	50	7	1	0	0	0	0	0	0	16	0	0	0	0	23
8-Aug-06	12	sparse	1/4	1	0	13	0	0	0	0	0	1	0	0	0	0	15
8-Aug-06	12	sparse	1/2	2	0	0	0	0	0	0	0	1	0	0	0	0	4
8-Aug-06	12	sparse	3/4	13	0	14	0	0	0	0	0	15	0	0	0	0	42
8-Aug-06	12	dense	50	0	0	20	0	0	0	0	0	2	0	0	0	0	21
8-Aug-06	12	dense	100	0	0	8	0	0	0	0	0	2	0	0	0	0	10
8-Aug-06	12	dense	150	7	1	0	0	0	0	0	0	0	0	0	0	0	8
9-Aug-06	18	open	150	2	0	5	0	0	0	0	0	22	0	0	0	0	33
8-Aug-06	18	open	100	2	0	1	0	0	0	0	0	26	0	0	0	0	29
8-Aug-06	18	open	50	1	0	15	0	0	0	0	0	16	0	0	0	0	32
8-Aug-06	18	sparse	1/4	0	0	0	0	15	0	0	0	3	0	0	0	6	23
8-Aug-06	18	sparse	1/2	0	0	0	0	0	0	0	0	8	0	0	0	3	11
8-Aug-06	18	sparse	3/4	5	0	24	0	0	0	0	0	2	0	0	0	0	31
9-Aug-06	18	dense	50	1	0	5	0	0	0	0	0	1	0	0	0	0	7
8-Aug-06	18	dense	100	2	1	10	0	0	0	0	0	0	0	0	0	0	13
9-Aug-06	18	dense	150	0	0	6	0	0	0	0	0	0	0	0	0	0	6
9-Aug-06	#6	creek	a	26	2	2	0	0	0	0	0	30	0	0	0	0	60
9-Aug-06	#6	creek	b	21	2	0	0	0	0	0	0	17	0	0	0	0	40
9-Aug-06	#6	creek	c	20	30	0	0	0	0	0	0	6	0	0	0	0	55
9-Aug-06	#27	creek	d	20	1	5	0	0	0	0	0	4	0	0	0	0	30
9-Aug-06	#27	creek	e	2	0	0	0	0	0	0	0	1	0	0	0	0	3
9-Aug-06	#27	creek	f	7	0	3	0	0	0	0	0	32	0	0	0	0	41
9-Aug-06	#18	creek	g	31	0	1	0	0	0	0	0	4	0	0	0	0	35
9-Aug-06	#18	creek	h	10	0	0	0	0	0	0	0	17	0	0	0	0	27
9-Aug-06	#18	creek	i	0	13	1	0	0	0	0	0	7	0	0	0	0	21

Table E-9. Existing fish density data.

Zone	Date	Site	Transect	# Traps	Fathead Minnow	White Bass	Green Sunfish	Carp	Bullhead	Crawdads	Mosquitofish
Dense	11-Aug-06	150 m	18"	4	1	4	0	0	0	0	0
Dense	11-Aug-06	100 m	18"	4	0	1	0	1	0	0	0
Dense	15-Aug-06	50 m	12"	4	0	0	0	0	0	0	244
Dense	15-Aug-06	100 m	12"	4	0	0	0	0	0	0	211
Dense	11-Aug-06	50 m	6"	4	1	0	0	0	0	0	0
Dense	11-Aug-06	100 m	6"	4	0	0	0	0	0	0	0
Sparse	11-Aug-06	3/4	18"	4	0	0	1	0	0	0	0
Sparse	11-Aug-06	1/4	18"	4	1	0	0	0	0	0	0
Sparse	15-Aug-06	3/4	12"	4	0	0	0	0	0	0	0
Sparse	15-Aug-06	1/2	12"	4	0	0	0	0	0	0	0
Sparse	11-Aug-06	1/4	6"	4	6	0	0	0	0	0	0
Sparse	11-Aug-06	3/4	6"	4	0	1	0	0	1	0	0
Open	11-Aug-06	50 m	18"	4	29	0	0	0	0	0	0
Open	11-Aug-06	150 m	18"	4	12	0	0	0	0	0	0
Open	15-Aug-06	50 m	12"	4	3	0	0	0	0	0	0
Open	15-Aug-06	100 m	12"	4	40	0	0	0	0	0	0
Open	11-Aug-06	50 m	6"	4	1	3	0	0	0	0	0
Open	11-Aug-06	150 m	6"	4	27	0	0	0	0	0	0
Creek	15-Aug-06	6	random	4	0	0	0	0	0	6	5
Creek	15-Aug-06	27	random	4	8	0	0	0	0	1	0
Creek	15-Aug-06	18	random	9	9	0	0	0	0	2	0
				Totals:	138	9	1	1	1	9	460

Appendix F Larval Drift Simulation

We conducted a larval drift simulation using neutrally buoyant pea-sized spheres obtained from Trina Hedrick of the Utah Division of Wildlife Resources. The simulation was conducted on July 17, 2006. Estimated discharge in Hobble Creek that day was 40 cfs. Three drift nets were suspended mid-way between the substrate and water surface to capture beads suspended in the water column. These nets were located 1.35, 2.0 and 2.4 km downstream from the input location (1600 W bridge in Springville). Figure F-1 depicts the reach of Hobble Creek where the larval drift simulation took place, and shows sample locations.

Once the beads were in the water of the creek it became apparent that they were actually negatively buoyant. Only a few (3-4) beads were found in the most upstream sample net, and none were observed in the nets located 2.0 and 2.4 km downstream. However, hundreds, if not thousands, of beads were observed tumbling along the streambed below the sample net at the most upstream sample location (1.35 km downstream from starting point). No beads were seen on the streambed at the other two sample sites.

Figure F-1. Reach of Hobble Creek showing where larval drift beads were put in to Hobble Creek and the three downstream sample nets.

Figure F-2. Drift bead sample net halfway between the streambed and water surface. This is the net located 2.4 km downstream from the starting location.

Appendix G Additional References

Bunte, K., Abt, S. (2001). "Sampling surface and sub-surface particle size distributions in wadable gravel- and cobble-bed streams for analyses in sediment transport, hydraulics, and streambed monitoring." Gen. Tech. Rep. RMRS-GTR-74. Fort Collins, CO: U.S. Department of Agriculture, Forest Service, Rocky Mountain Research Station. 428 p.

Rosgen, D. (1996). *Applied River Morphology*. Wildland Hydrology, Pagosa Springs CO.